Computer Modelling of Biomaterials: Hydroxyapatite, Collagen and Bioglasses

Nora de Leeuw

Department of Chemistry
University College London, UK

Biominerals

Composite materials made up of inorganic mineral phase formed at organic templates, which direct growth into highly specific structures/morphologies

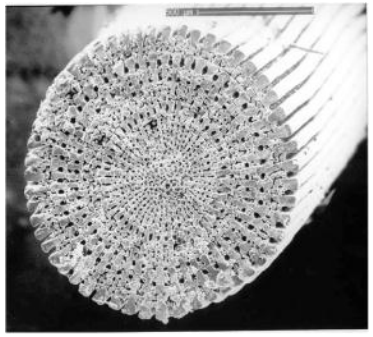

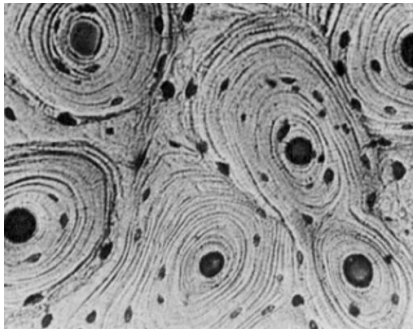

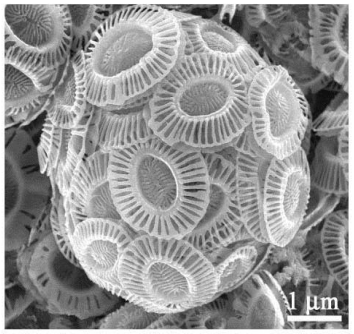

Natural Bone

- Important natural composite material
- Relatively simple protein phase (collagen I)
- Mineral phase (hydroxyapatite)
- Interaction with experiment
  - Validation of models
  - Interpretation of experiment, e.g. NMR
- Applications to e.g.:
  - Osteoporosis and other bone disorders
  - Bio-compatibility of metal/glass/ceramic implants

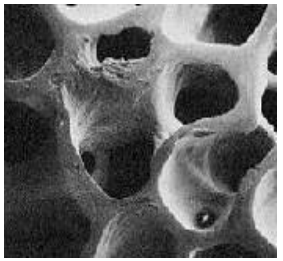

Normal bone

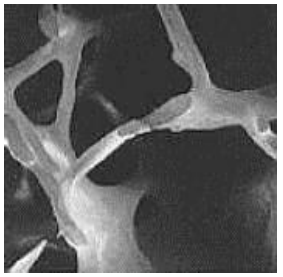

Osteoporotic bone

Multiple Levels of the Bone Structure

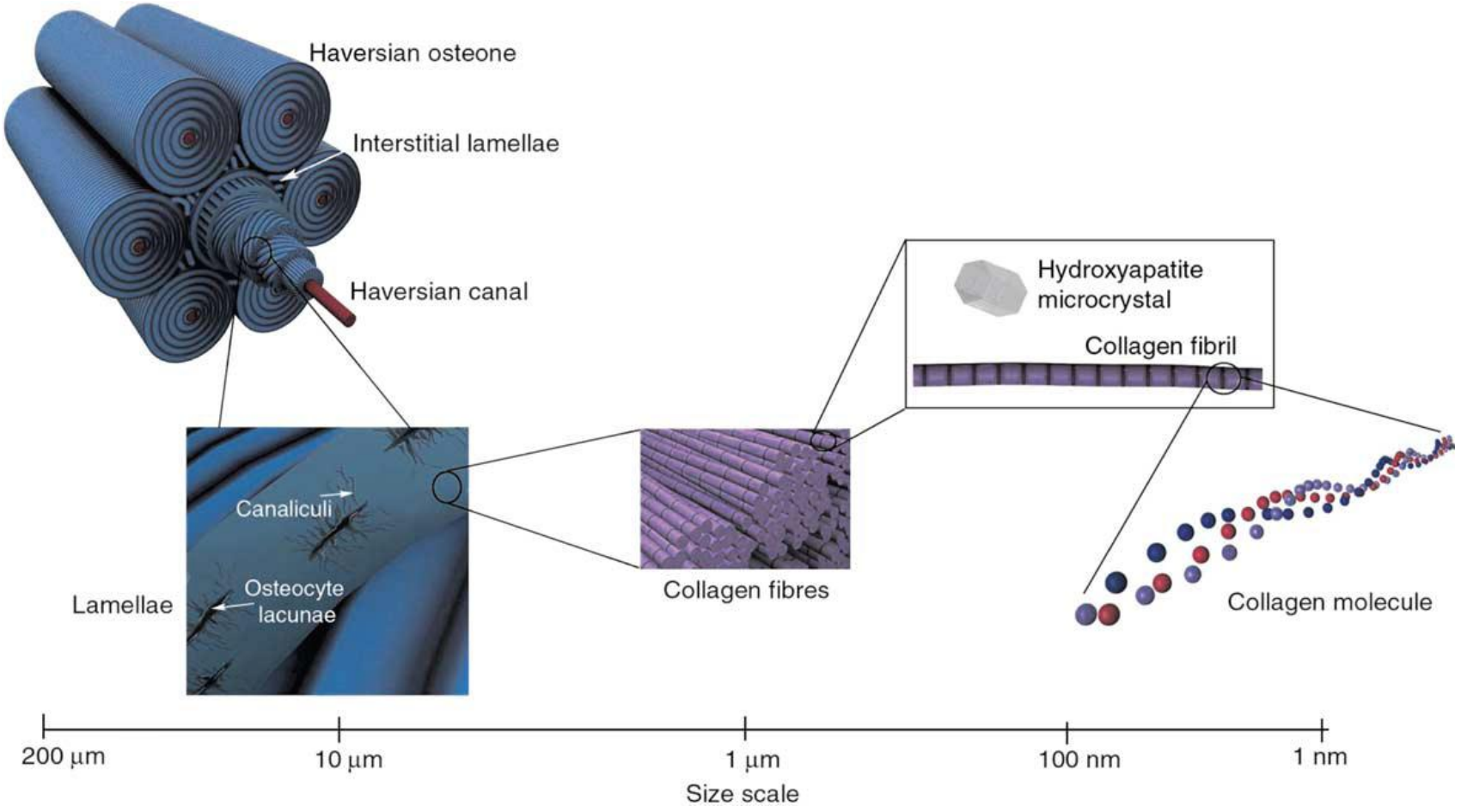

Collagen Type I

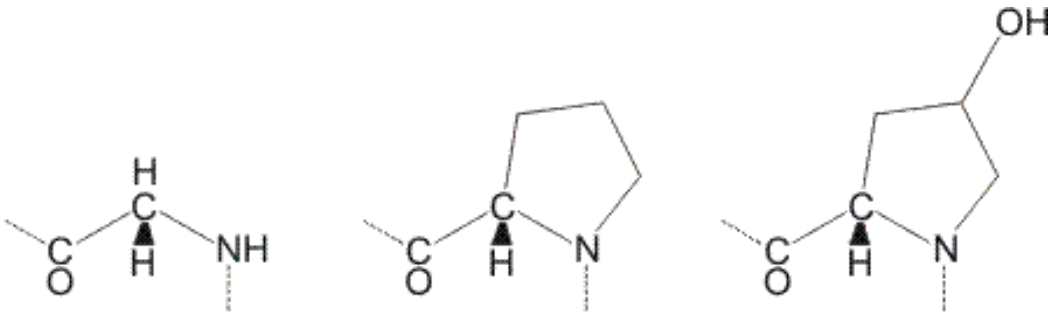

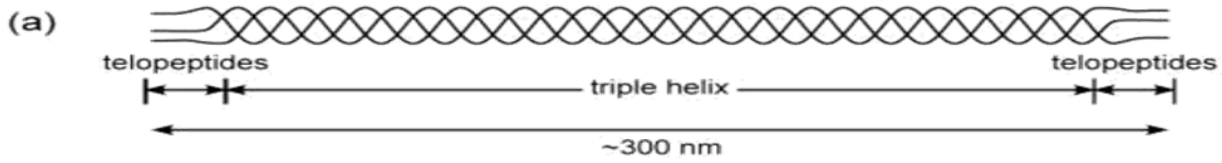

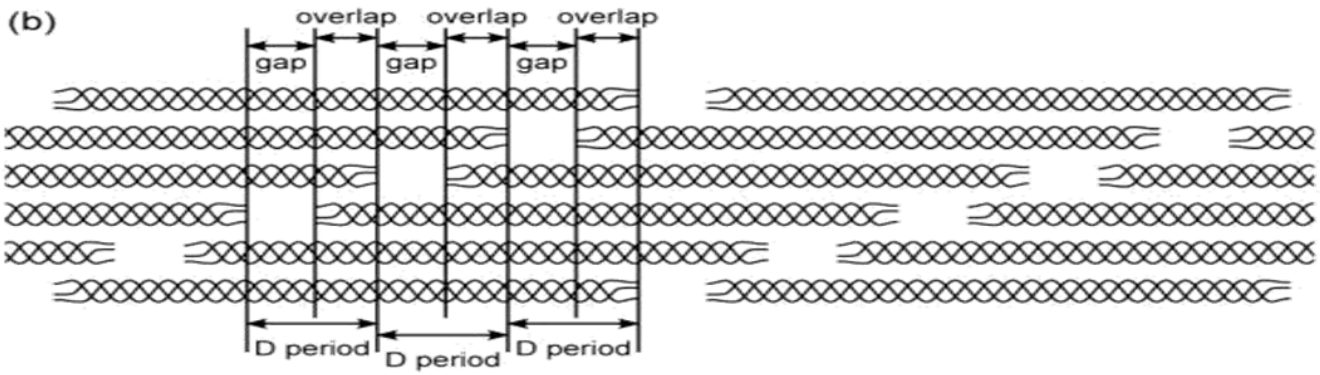

Mineralised collagen

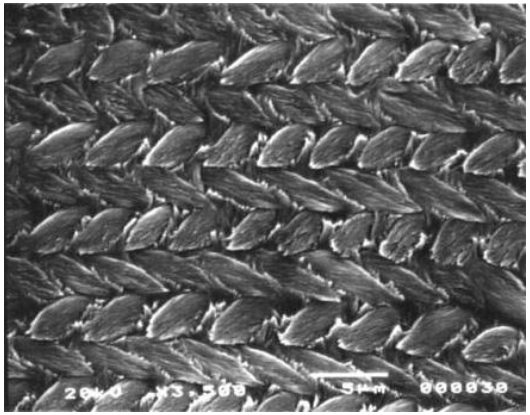

SEM of mouse tooth enamel

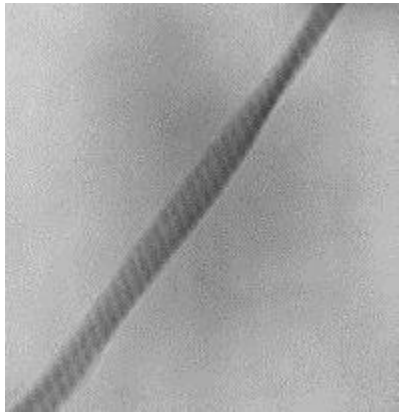

Electron micrograph of collagen banding

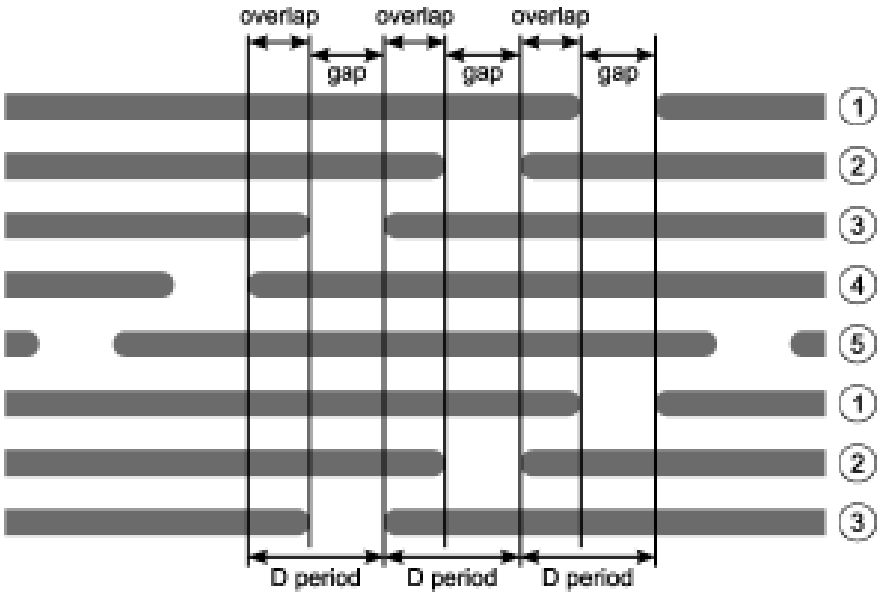

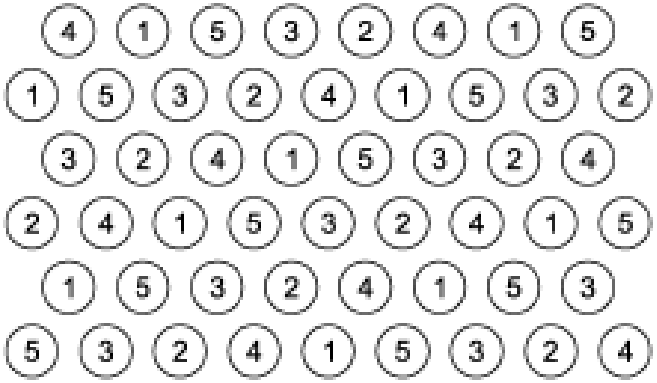

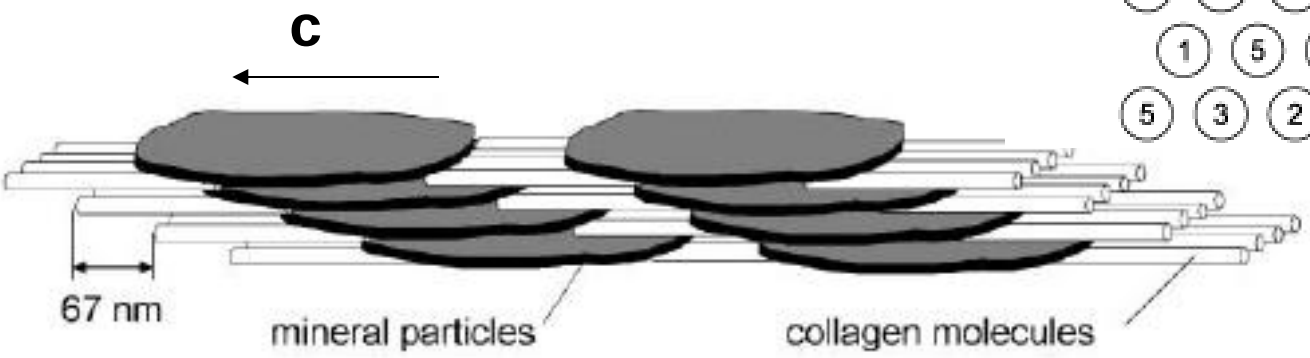

Scientific Issues

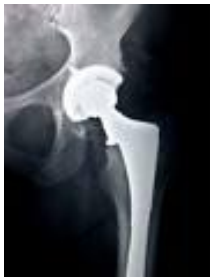
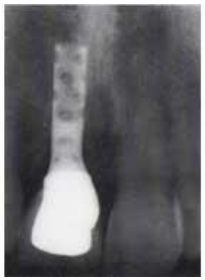
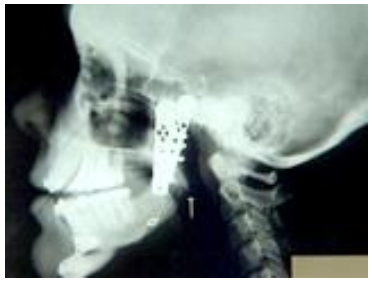

- Bio-mineralisation of organic/inorganic composites (bone, teeth, shells)
- Design & integration of bio-active glass/ceramic implants

BUT

- Difficult to obtain molecular-level insight using experimental techniques
- Computational research can help enormously, although:
  - Gap between experiment and computation
  - Gap between biology/medicine and physical sciences/engineering

Challenge for Computational Research

- Need for high accuracy but also large systems
  - Bridging length- and time-scales
- Need to match models for complex bio-molecules with methods for materials simulation
  - Protein modelling is well advanced subject
  - Materials simulation now highly accurate and reliable
- Need to scale up models for direct comparison with experiment, without loss of molecular-level information

Methodology

- Ab initio methods
  - Geometry optimisation: Siesta, VASP
  - Molecular Dynamics: Quatum Espresso, CP2K
- Classical Interatomic Potential methods
  - Molecular Dynamics: DL_POLY, Amber

Ab initio –v– Classical simulations of glasses

	classical	*ab initio*
size	10^3-10^4 atoms	10^2 atoms
melt	6000 K	2500-3000 K
cooling rate	1 K ps^{-1}	50 K ps^{-1}
300 K	*O*(ns)	*O*(10 ps)
wall time	days	months

classical: DLPOLY

ab initio: CP2K & Q-ESPRESSO, GGA, PBE funcs., Γ-point only

SIESTA calculations of adsorption of glycine, proline and hydroxy-proline to HA surfaces

Glycine

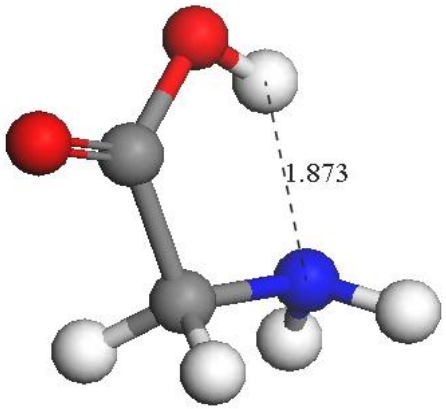

Proline

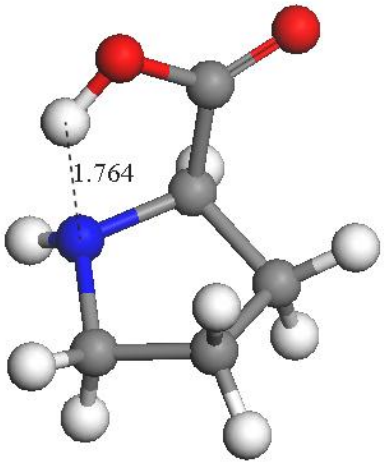

Hydroxyproline

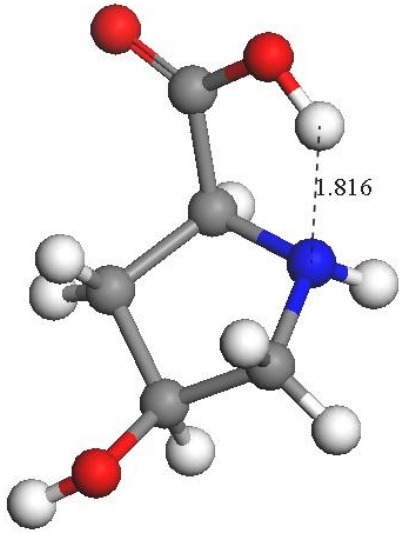

Hydroxyapatite $Ca_{10}(PO_4)_6(OH)_2$

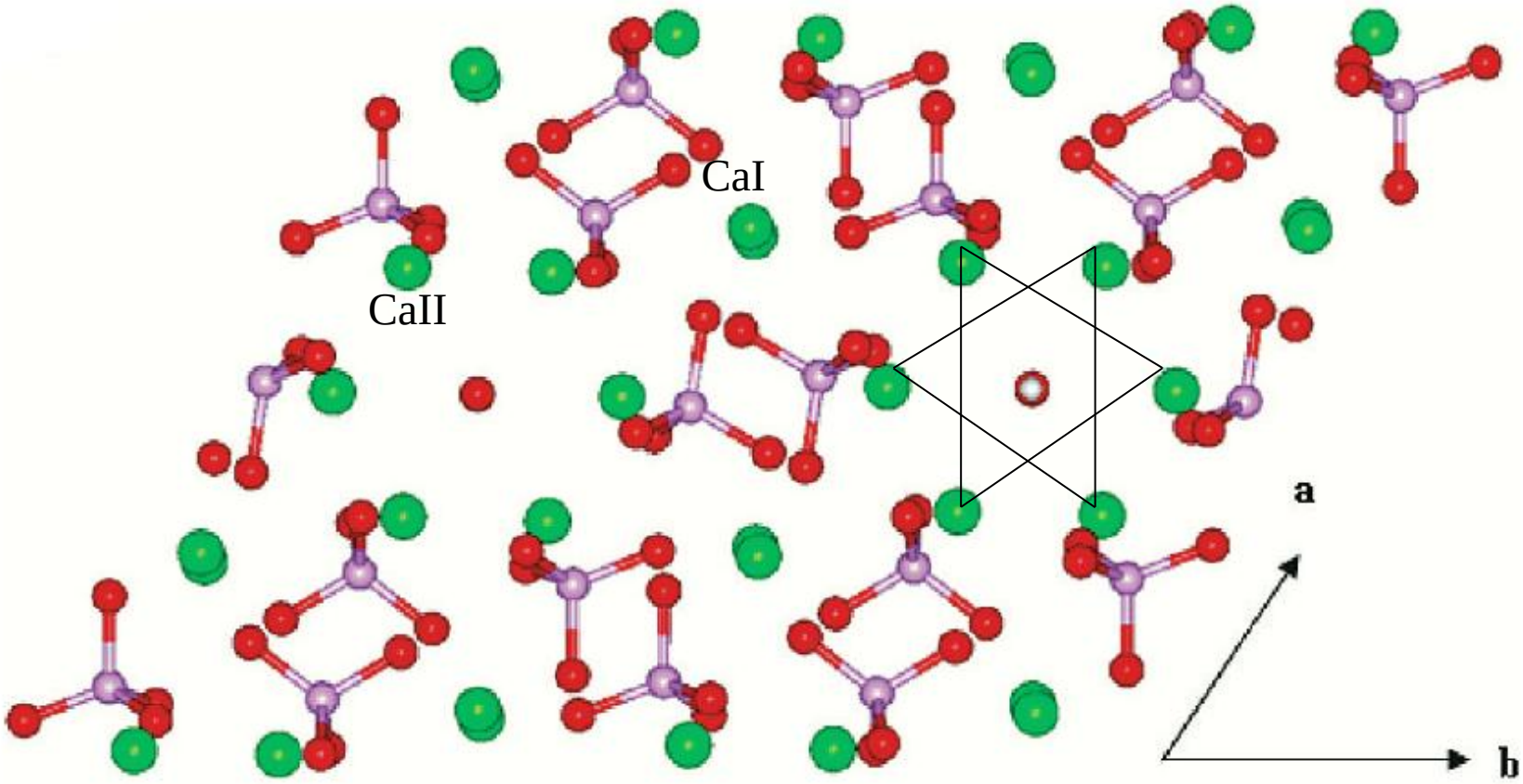

Surface stabilities

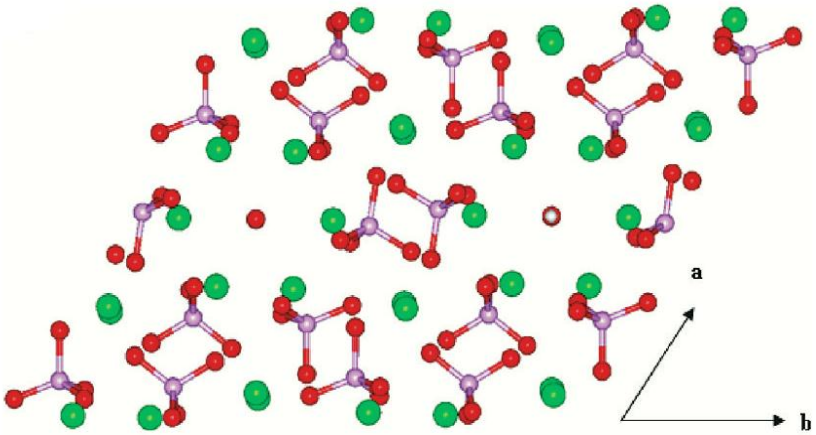

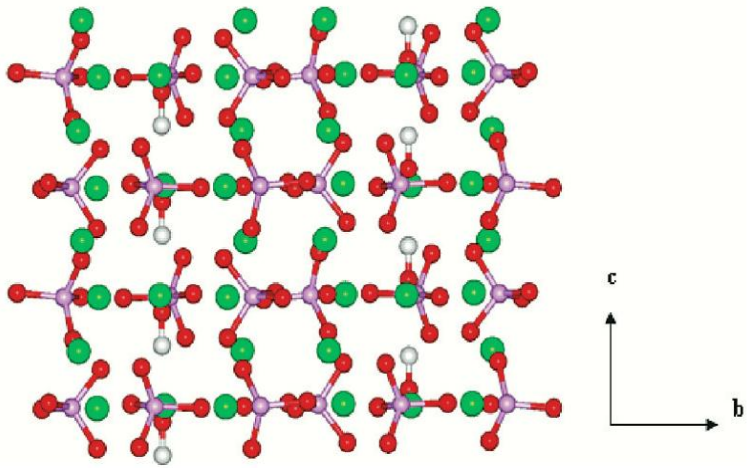

$$\gamma = (E_{surf} - E_{bulk}) / A$$

A low positive γ indicates a stable surface

Comparison of surface energies γ (Jm^{-2}) calculated from different methods				
Surface	Termination	Siesta	DL_Poly in vacuo	DL_Poly in water
(0001)	PO_4-Ca-PO_4-PO_4-Ca-Ca	0.94	0.91	0.37
(01.0)	Ca-Ca	1.27	1.23	1.90

M.R.T. Filgueiras, D. Mkhonto, N.H. de Leeuw, *J. Cryst. Growth* (2006) **294**, 60.

Hydrated apatite surfaces

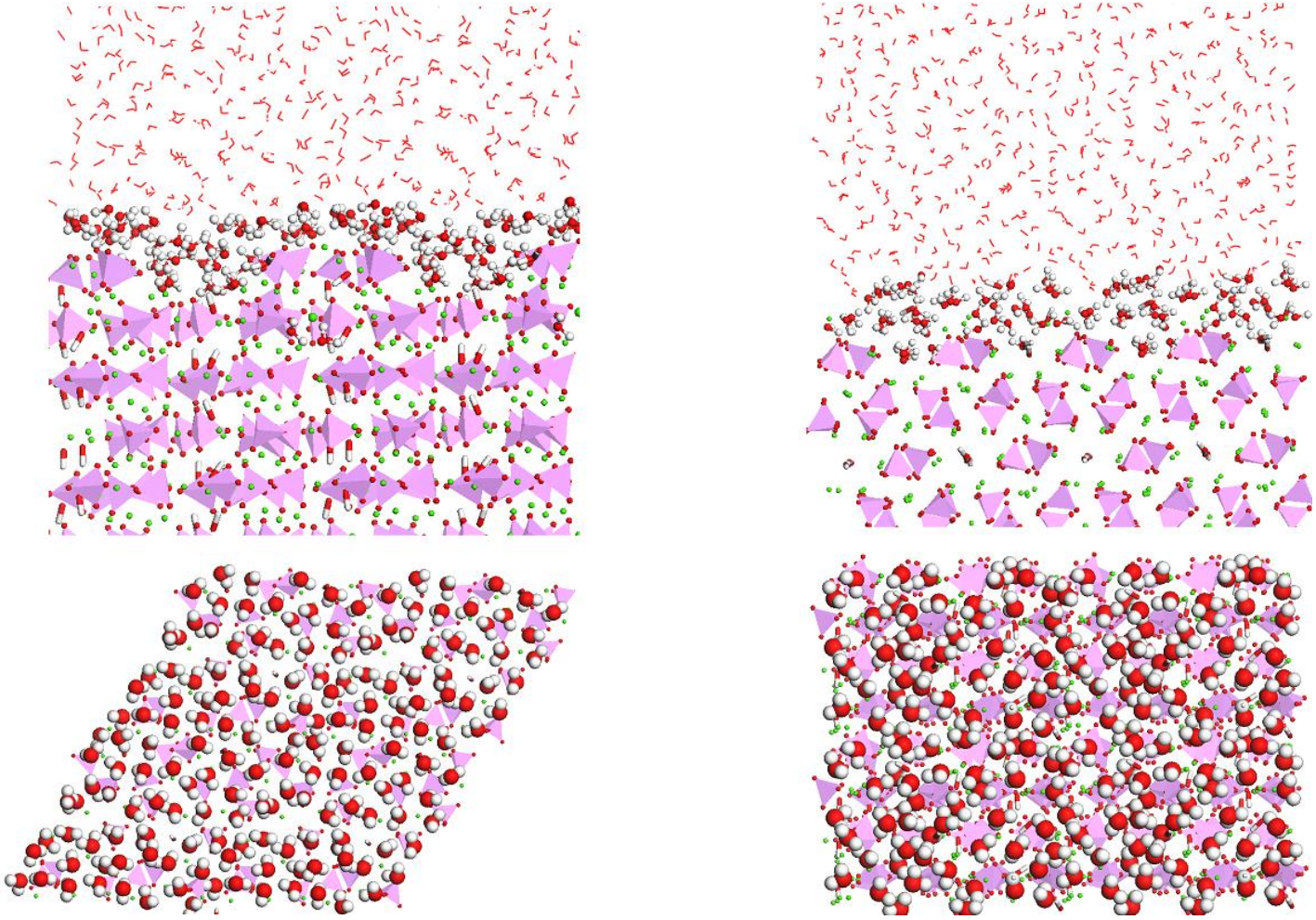

(0001) (01.0)

N.H. de Leeuw, J.A.L. Rabone, *CrystEngComm.* (2007) **9**, 1178.

Interfacial water structure

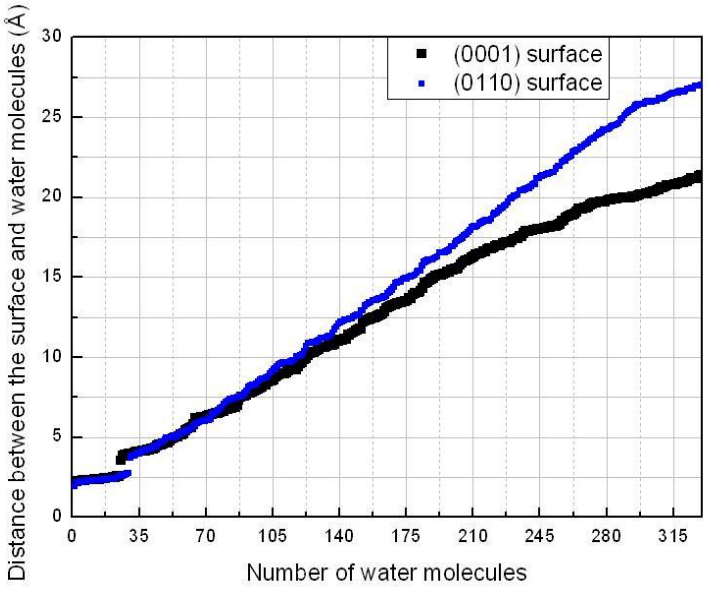

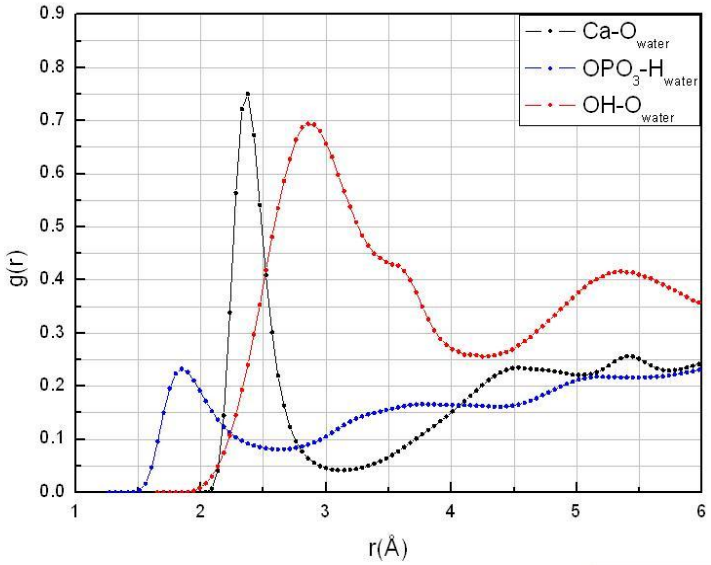

- Irregular pattern of adsorbed water
- First water layer close to surface (4 Å), in agreement with experiment and earlier simulations
- No long-range order
- Ca-O_w, O_{PO4}-H_w, H_{OH}-O_w in agreement with ab initio MD calculations of hydrated ions

E. Tang, D. Di Tommaso, N.H. de Leeuw, *J. Chem. Phys.* (2009) **130**, 234502.

Adsorption of amino acids at HA surfaces

(0001)

(01$\bar{1}$0)

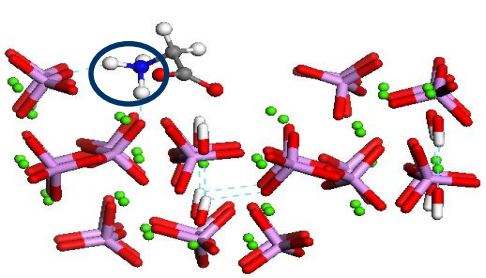

Glycine

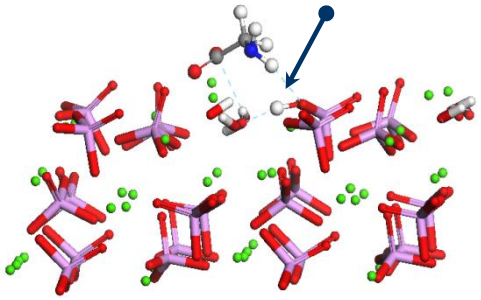

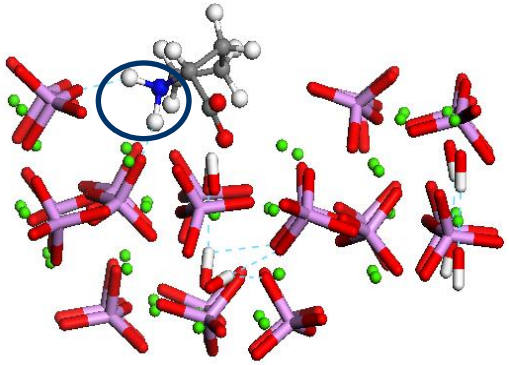

Proline

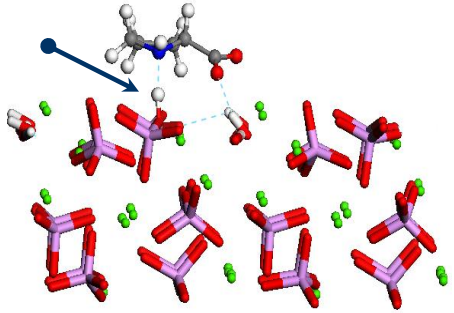

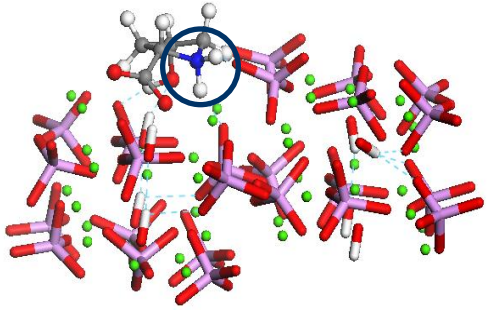

Hydroxyproline

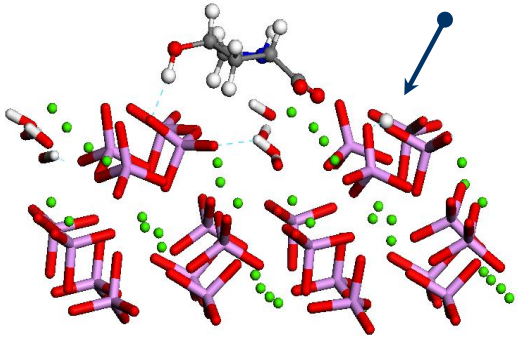

Binding Strengths

$$E_{ads} = E_{syst} - \left(E_{surf} + E_{a.a.} \right)$$

Adsorption energies (kJ mol^{-1})			
HA Surface	Glycine	Proline	Hydroxyproline
(0001)	-291.0	-322.3	-507.7
(01$\bar{1}$0)	-496.6	-554.5	-609.8

- All amino acids form multiple interactions with surface species, particularly if they can bridge between two surface calcium ions
- Strong interactions with surfaces, involving changes in chemical bonding
- Glycine more flexible but less adhesive
- Binding to (01$\bar{1}$0) surface stronger for all three adsorbates

N. Almora-Barrios, K. F. Austen, N. H. de Leeuw, *Langmuir* (2009) **25**, 5018.

Adsorption of tri-peptide

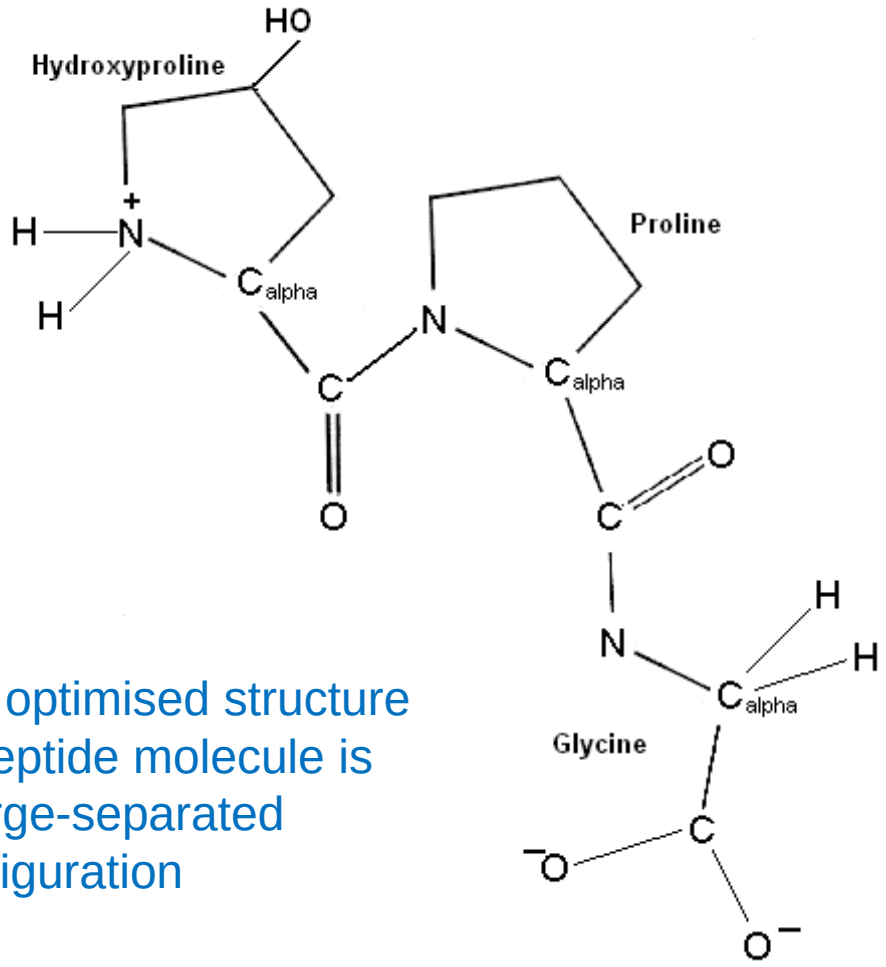

The optimised structure of peptide molecule is charge-separated configuration

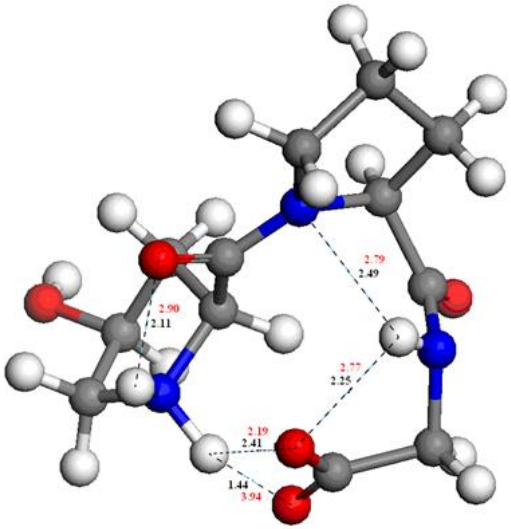

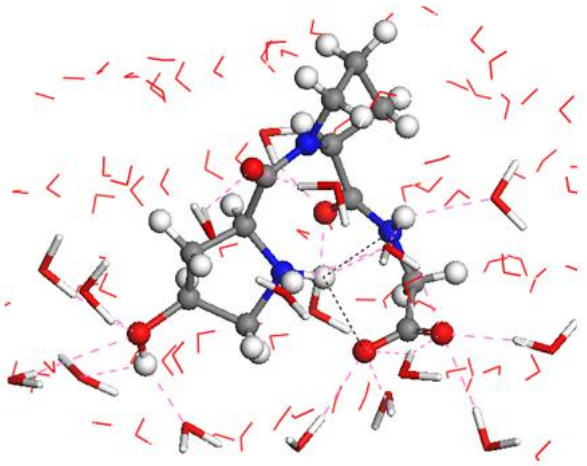

Peptide surface interactions *in vacuo*: DFT -v- MD

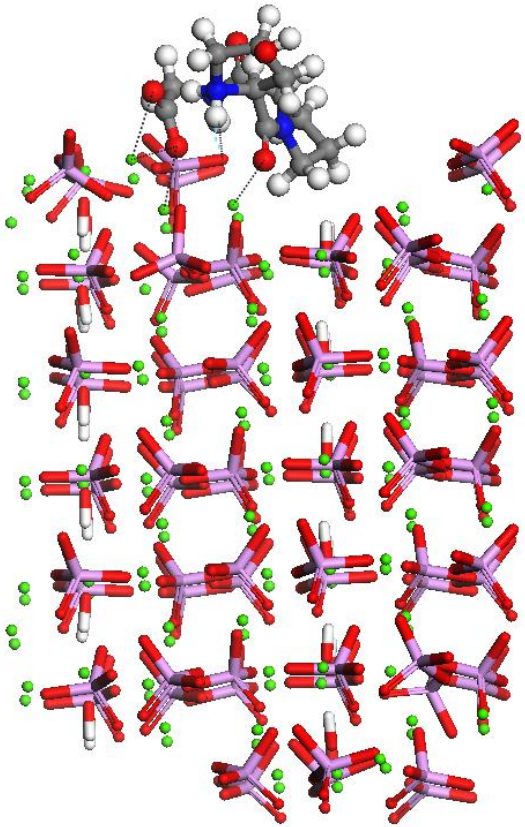

(0001)

Adsorption energies (kJ mol^{-1})			
HA surface	DFT in *vacuo*	MD in *vacuo*	MD in water
(0001)	-429.6	-470.8	-157.4
(01$\bar{1}$0)	-636.5	-604.5	-680.6

Both methods lead to similar geometries:

- Primary association via Ca^{2+} – COO^- interaction.
- Closer contact at (0001) surface

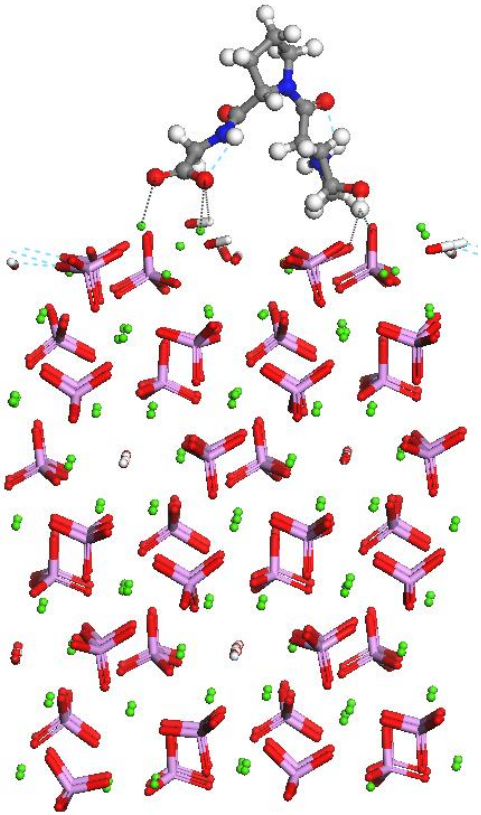

(01$\bar{1}$0)

MD simulations in aqueous environment

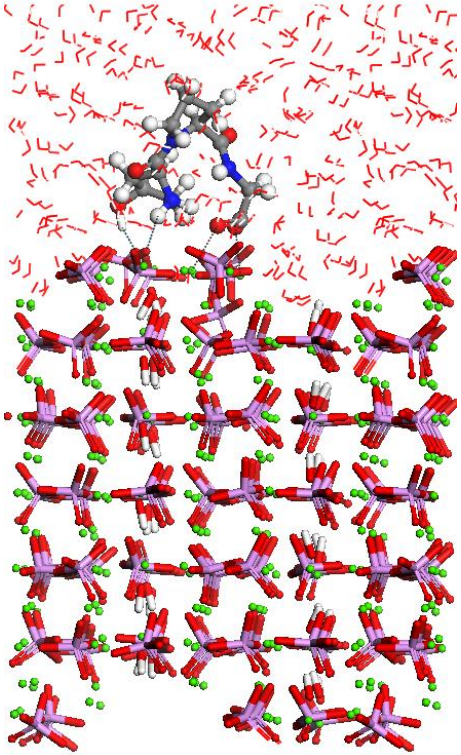

(0001)

- Weaker adsorption of peptide at (0001) surface compared to dry surface.
- Competitive adsorption of water moderates adsorption: Water stabilises surfaces
- Peptide preferred over water at (01$\bar{1}$0) surface: good match between surface and adsorbate
- In the presence of collagen, the HA crystal should grow faster along (0001) than along (01$\bar{1}$0)

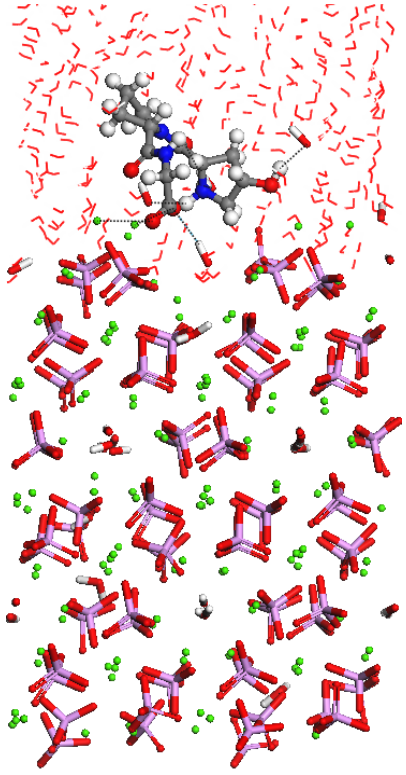

(01$\bar{1}$0)

NPT, temperature 310 K and a water density of 0.9922 g/mL

N. Almora-Barrios, N.H. de Leeuw, *CrystEngComm* (2010) **12**, 960.

HA Nucleation at tropocollagen molecule

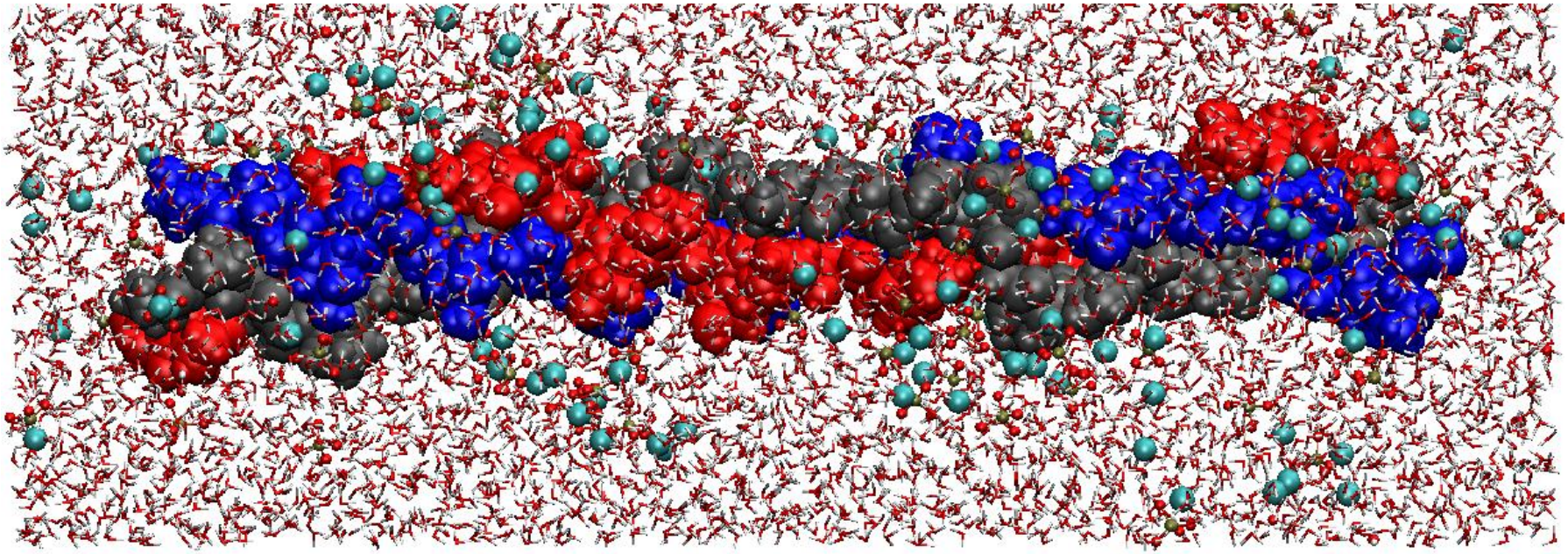

Triple helix of three chains of $[Gly\text{-}Pro\text{-}Hyp]_{10}$

120 Ca^{2+}, 72 PO_4^{3-}, 24 OH^-

ρ_{water} = 0.9922 g/mL, NPT (T = 310 K)

Hydration shells of Ca and PO_4

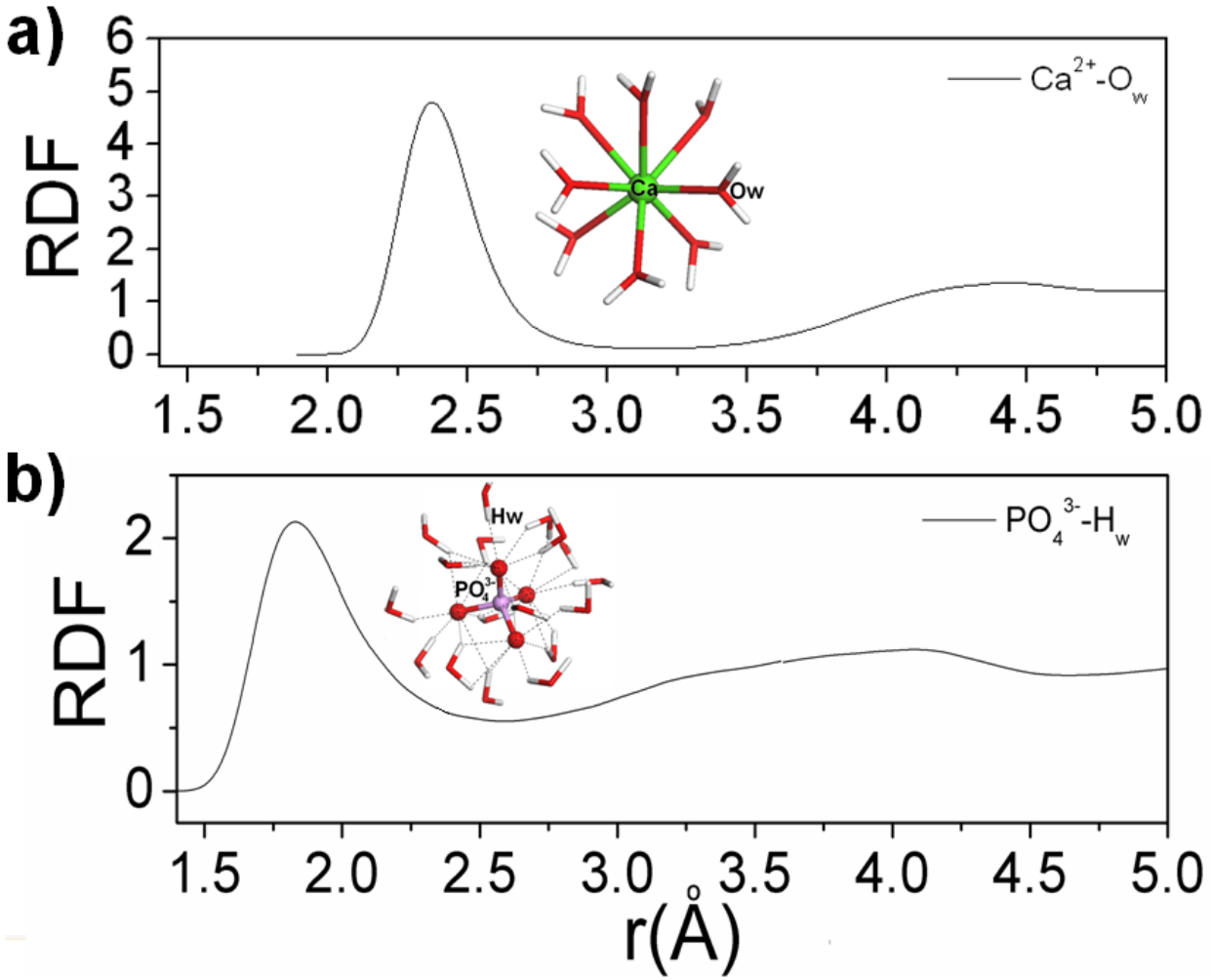

Agreement with experiment and *ab initio* MD calculations

Spontaneous Ion pairing

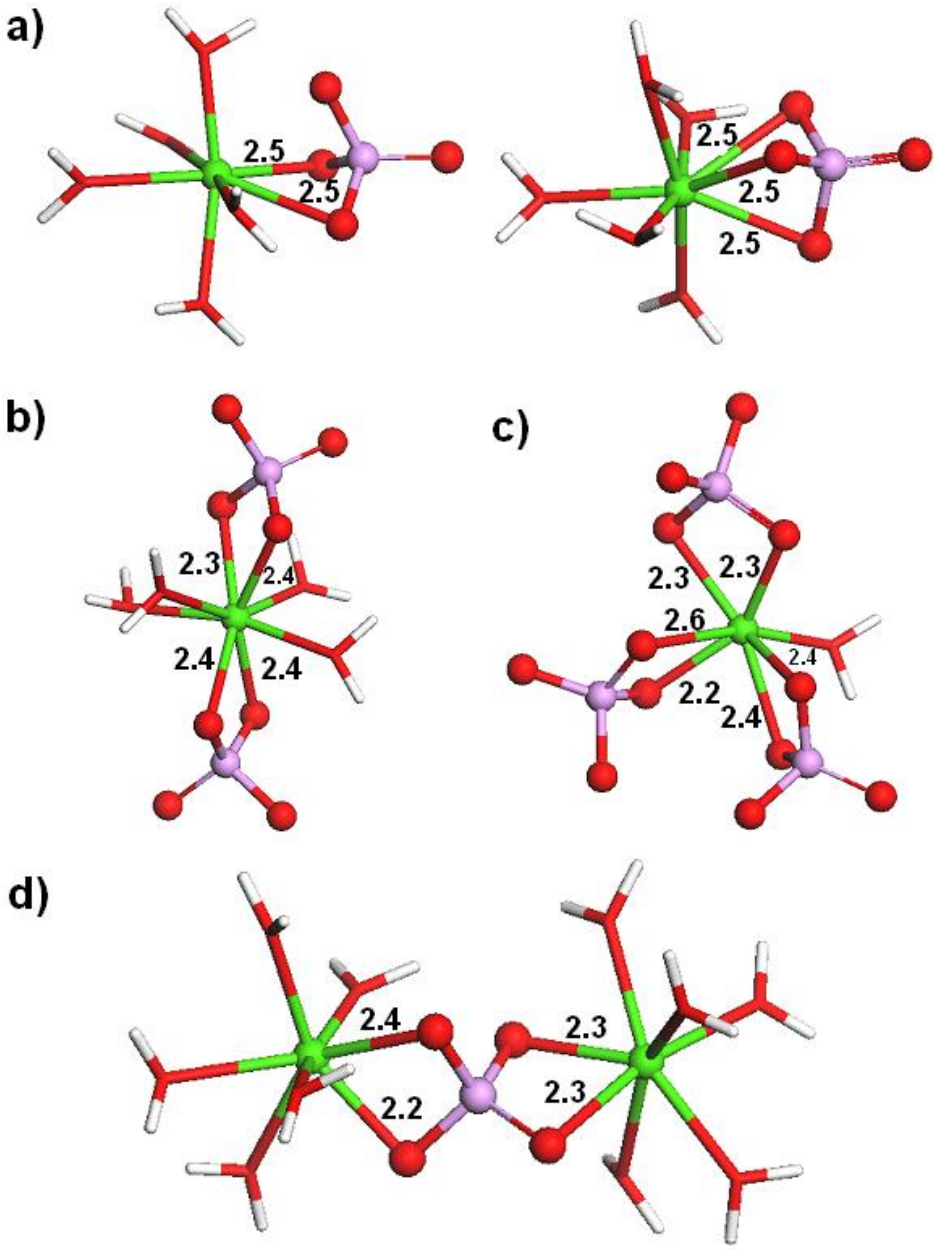

Coordination behaviour

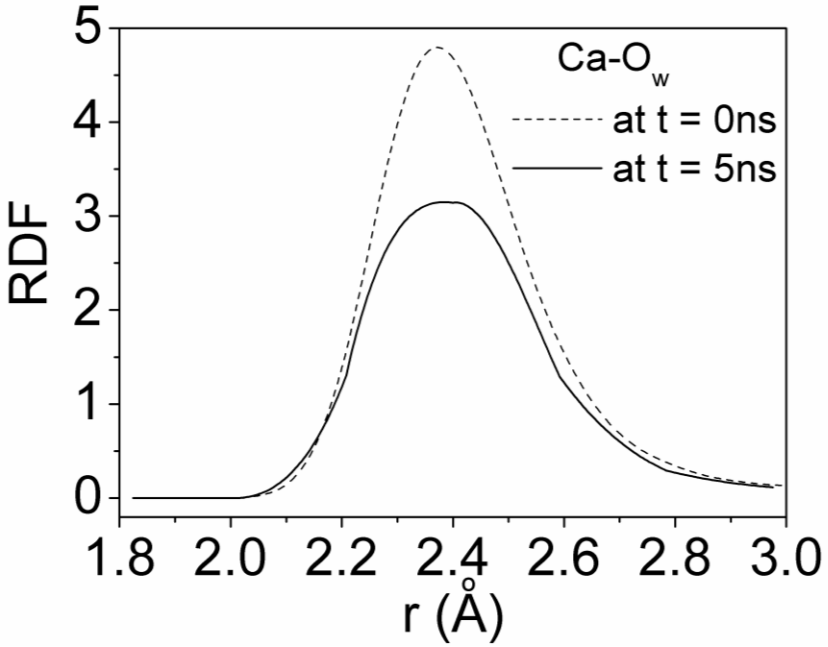

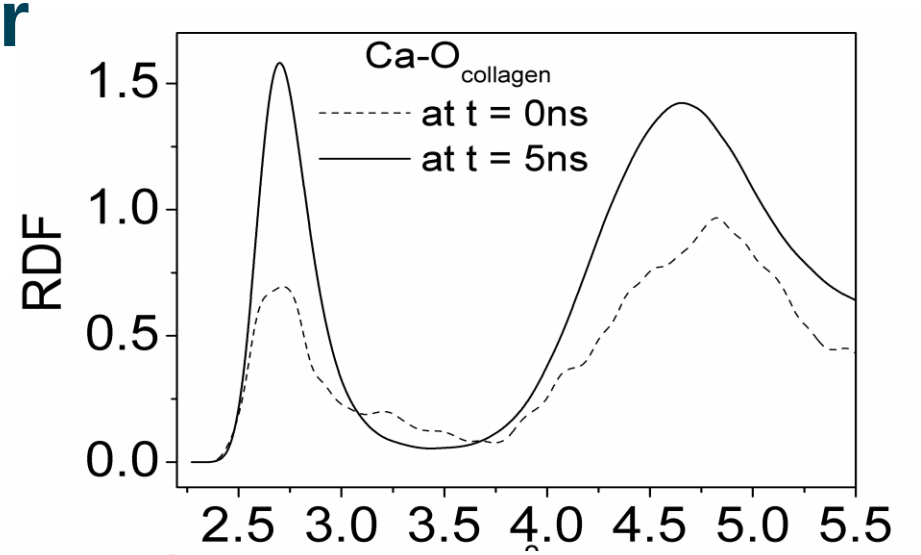

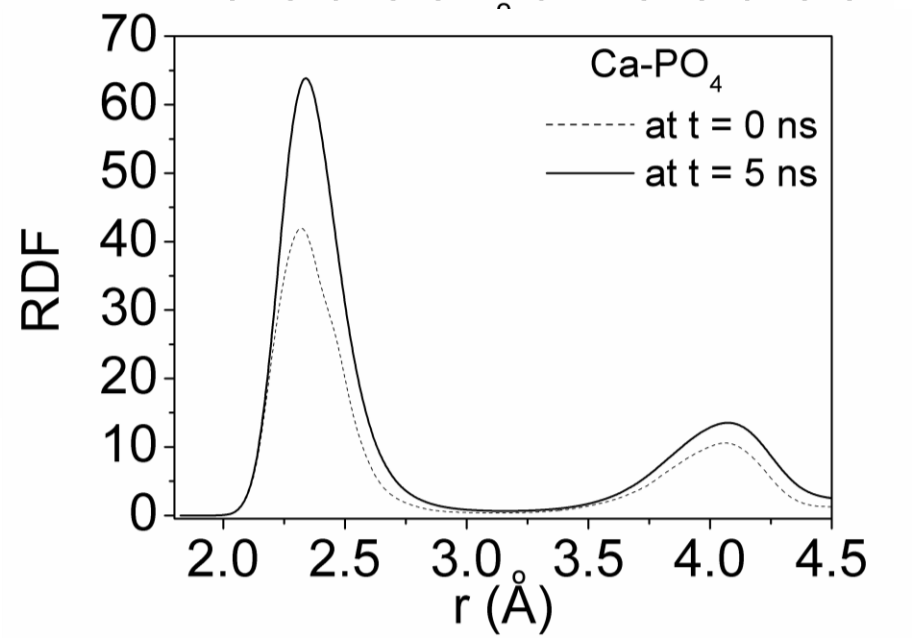

Formation of Calcium Phosphate Clusters

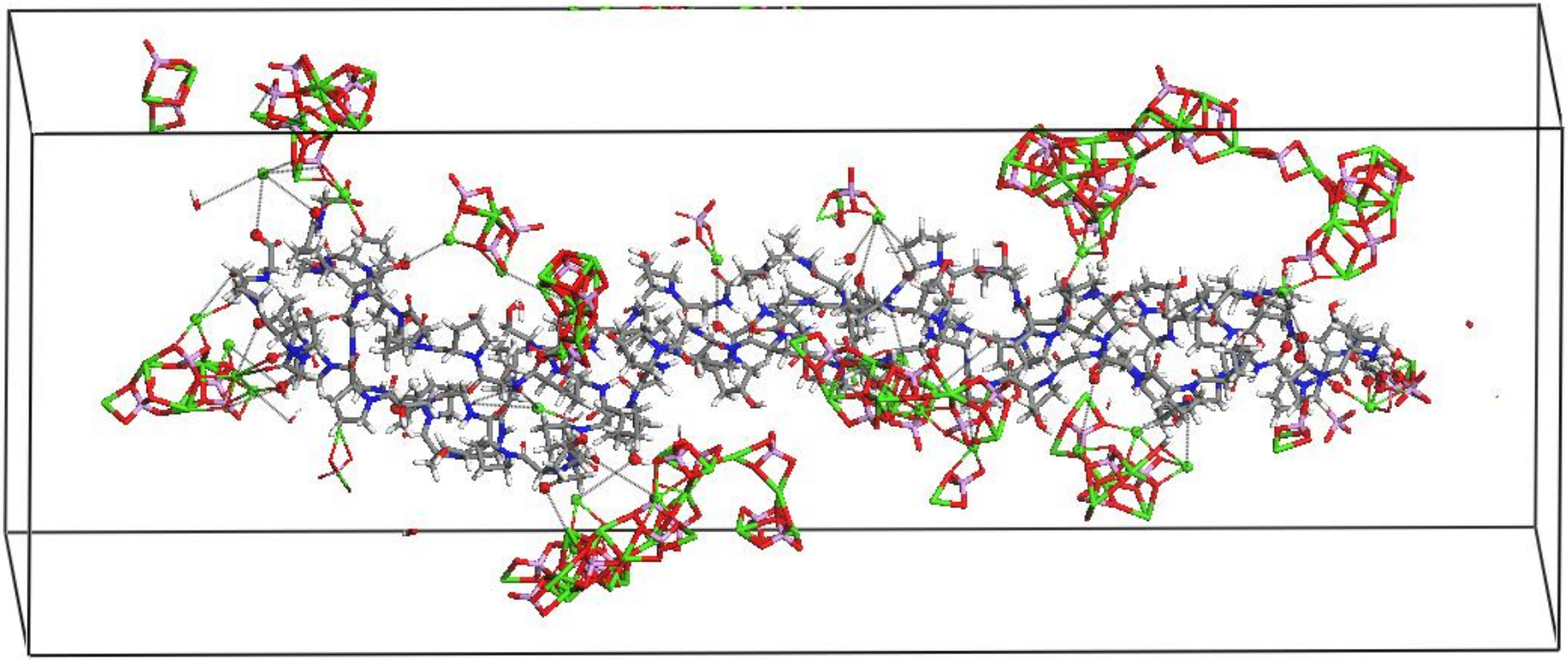

Snapshot of the system at 5 ns.

Trends from HA nucleation

- Ca strongly coordinates to collagen oxygen ions in C=O groups, but also OH
- Phosphate groups do not interact easily with collagen – some to HO of Hyp
- OH do not coordinate to collagen or calcium phosphate clusters
- Agrees with suggestion that amorphous CaP forms before crystallising into octa-calcium phosphate and hydroxyapatite

Collagen Simulations

- Structure from low-resolution X-ray study
- One tropocollagen per unit cell
- 11980 water molecules

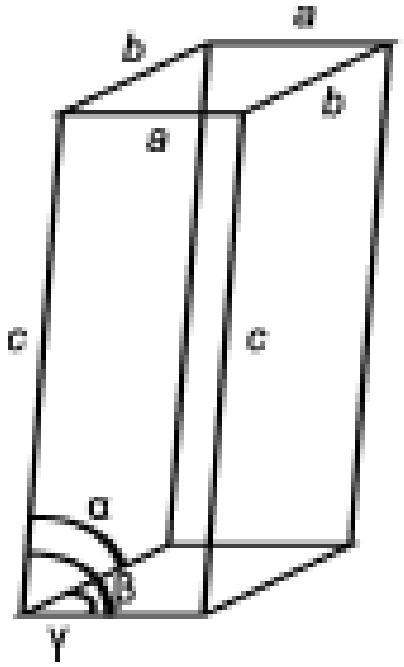

a=39.97 Å

b=26.95 Å

c=677.90 Å

$\alpha=89.24^0$

$\beta=94.59^0$

$\gamma=105.58^0$

Modelling the 3-D Collagen Matrix

- 300nm collagen molecules
- Complete peptide sequence
- Quasi-hexagonal packing
- Reproduces experimental structure and water content

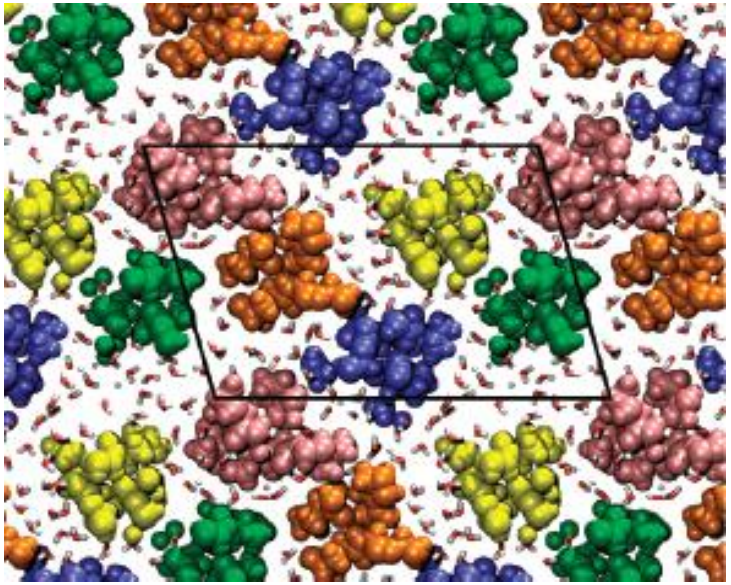

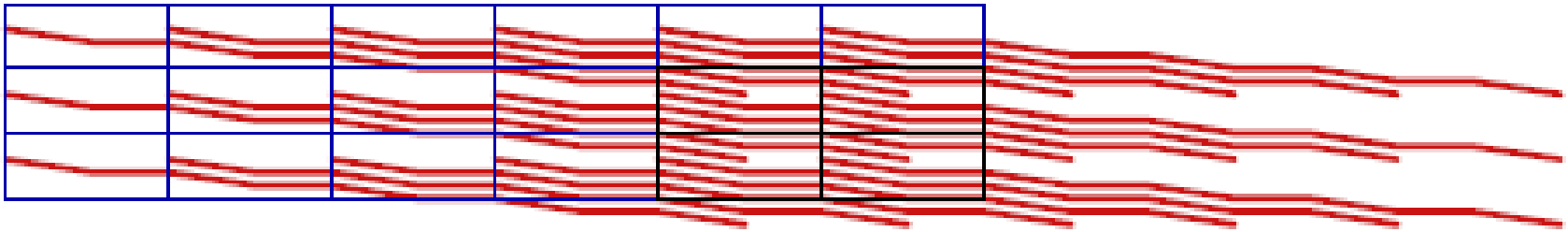

I. Streeter, N.H. de Leeuw, *J. Phys. Chem. B* (2010) **114**, 13263.

Inter- and intra-fibril interactions

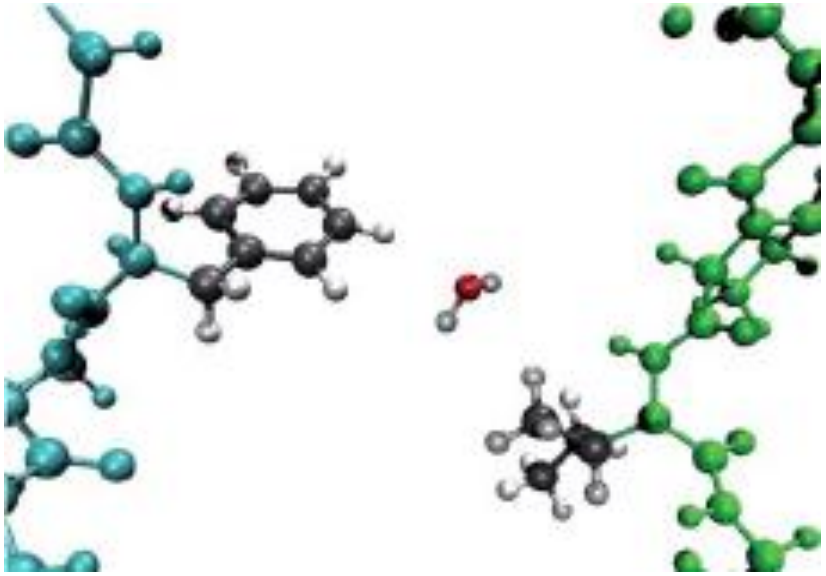

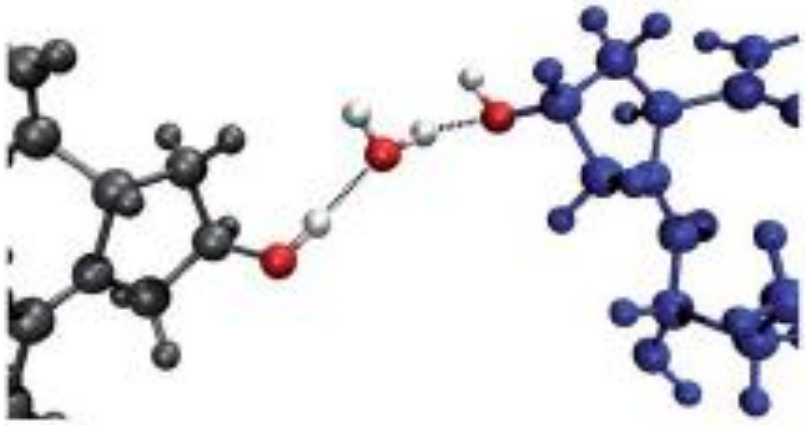

- Direct H-bonding
- Water bridges
- Hydrophobic interactions

H-bonded interactions in collagen –v– globular proteins

	Collagen fibril interprotein hydrogen bonds	Collagen fibril interprotein water bridges	Folded globular proteins intramolecular hydrogen bonds[10]
R:R	122.6 (62.6%)	53.9 (33.0%)	10.6%
N:R	19.4 (9.9%)	30.4 (18.6%)	10.4%
R:O	48.4 (24.7%)	62.4 (38.3%)	10.9%
N:O	5.6 (2.8%)	16.5 (10.1%)	68.1%
total	196.0	163.1	

R:R side chain to another side chain
(N:R) backbone N to a side chain
(R:O) side chain to a backbone O
(N:O) backbone N to a backbone O

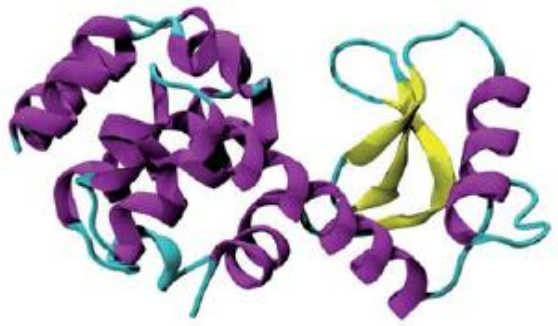

Lysozyme

Trends from pure collagen fibril calculations

- Polar groups at centre of fibril are in contact with relatively large quantities of intra-fibrillar water
- Little tendency to form protein–protein hydrogen bonds
- Majority of inter-molecular H-bonds are interactions between side chains
- The process of collagen fibrillogenesis acts to shield hydrophobic side chains from water molecules, but this effect is small

I. Streeter, N.H. de Leeuw, *Soft Matter* (2011) **7**, 3373.

Glucosepane Cross-Linking

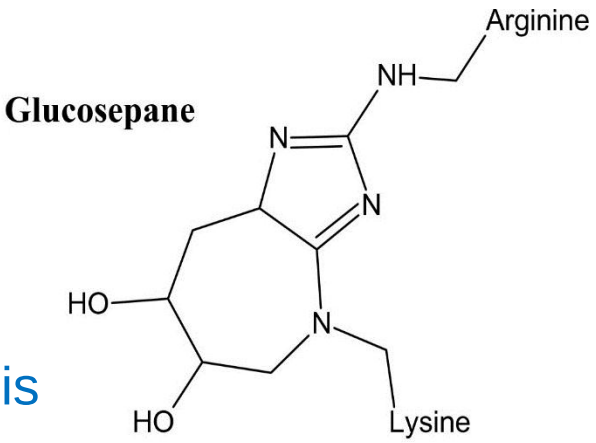

- Glucosepane cross-links form between a Lysine and an Arginine residue
- Glucosepane has been linked to the pathogenesis of several chronic diseases
- Believed to play a significant role in ageing with evidence proving its role in the stiffening of the extracellular matrix of lung and vascular tissue
- Experimental studies show that the Young's modulus of a rabbit Achilles tendon increase by on average 159% with the presence of glucosepane cross-links
- On average in healthy humans 1 in 5 collagen molecules is cross-linked; in sufferers of *diabetes mellitus this increases to 1 in 2*
- Currently no clinically licenced treatment or cure available

Impact of Glucosepane Cross-linking

- Glucosepane has been linked to the pathogenesis of several chronic diseases from neurodegenerative diseases to cancer metasis
- Believed to play a significant role in ageing with evidence proving its role in the stiffening of the extracellular matrix of lung and vascular tissue
- Experimental studies show that the Young's modulus of a rabbit Achilles tendon increase by on average 159% with the presence of glucosepane cross-links
- On average in healthy humans 1 in 5 collagen molecules is cross-linked in sufferers of *diabetes mellitus this increases to 1 in 2*
- Currently no clinically licenced treatment or cure available

Distance Based Criterion Search

- Distance Criterion: 5Å
- Conducted in VMD
- Measured at the three points shown.
- 24 Positions Identified

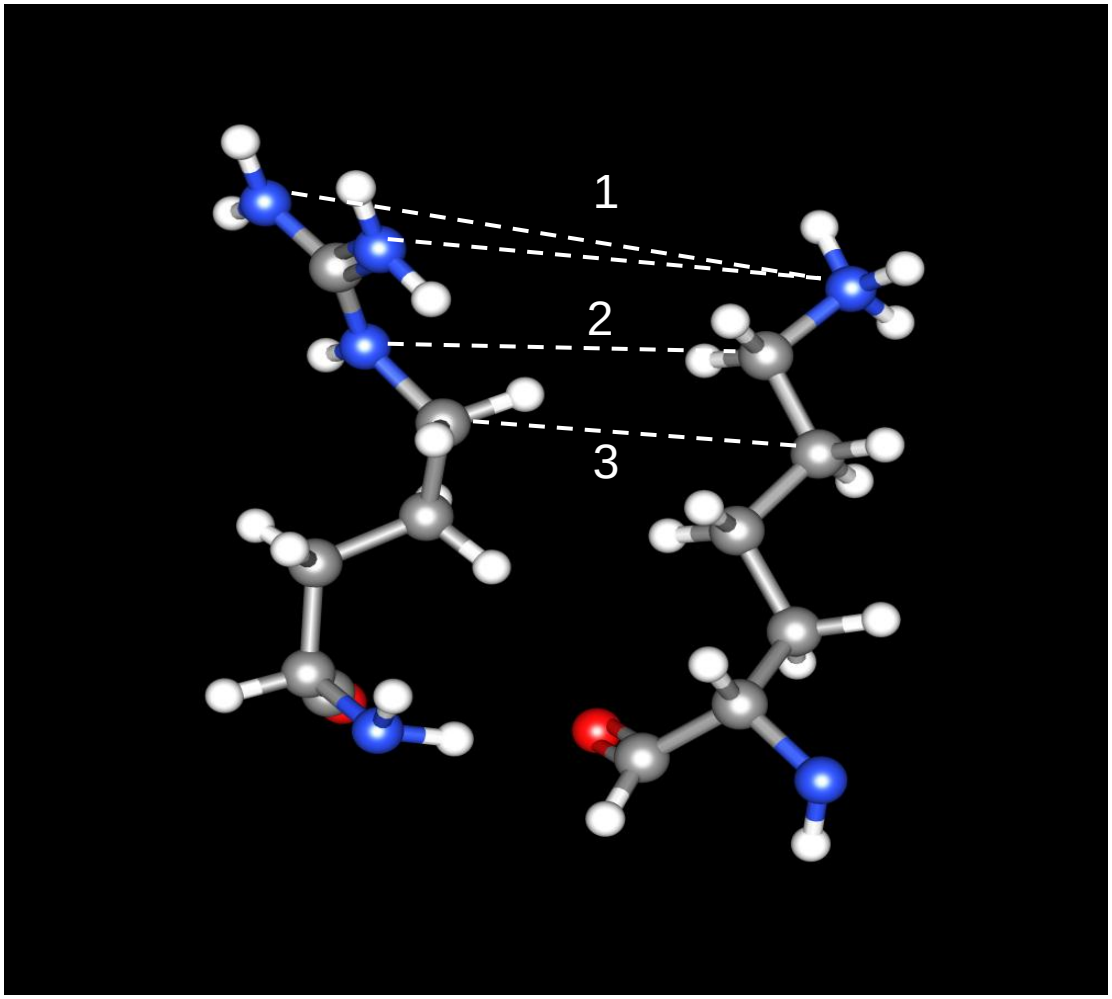

Distribution Of Potential Cross-linking Sites

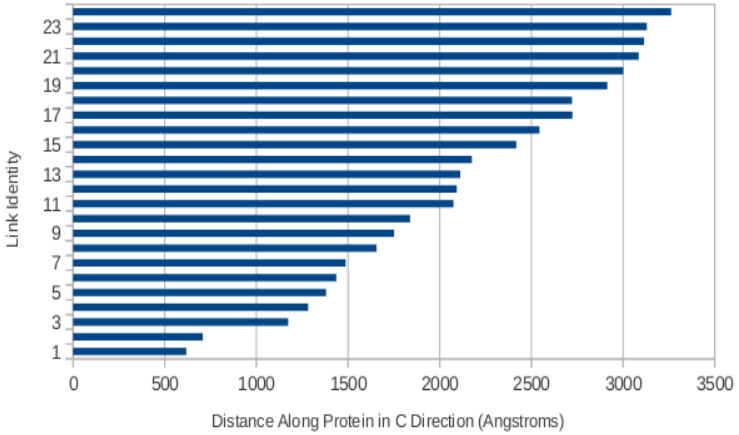

- Regions 1 & 4 average composition
- Region 2 high Lyz composition
- Region 3 incorporates an α-turn

Table 3.1: Percentage Composition of Protein Regions With No Binding Present.

Region of Collagen Protein	Lys (%)	Arg (%)	Lyz (%)	Gly (%)	Pro (%)
Whole Protein	3.2	5.0	0.3	33.1	10.9
Region 1	2.8	4.5	0	33.6	9.7
Region 2	0.9	5.7	0.9	34.1	7.4
Region 3	4.2	2.7	0	33.4	14.4
Region 4	2.8	6.9	0	33.2	7.4

Results

- 13 Positions with Endothermic Binding Enthalpy
- 11 Positions with Exothermic Binding Enthalpy

Table 3.2: Binding Enthalpy for a Single Glucosepane Cross-link.

Link	Arg Residue ID	Lys Residue ID	Binding Enthalpy (kcal/mol)
1	78	2171	+1091.790
2	2202	1154	-14.016
3	1319	2364	+12.983
4	307	1357	-39.568
5	1390	2439	+72.53
6	1409	358	+2.195
7	1427	376	-21.780
8	436	1487	+35.702
9	469	1520	+0.032
10	1550	2591	-91.253
11	583	2676	+11.582
12	1640	589	-37.433
13	1648	597	+65.406
14	1670	2715	+20.020
15	703	2796	+14.844
16	1796	745	-55.587
17	2901	807	-72.103
18	1856	2903	-40.261
19	874	2967	-21.528
20	904	1951	-0.339
21	3027	934	-50.759
22	943	1991	+67.705
23	949	2000	+1660.284
24	2044	990	+56.820

Position 1

- +1091.79 kcal/mol
- Highly Strained Structure

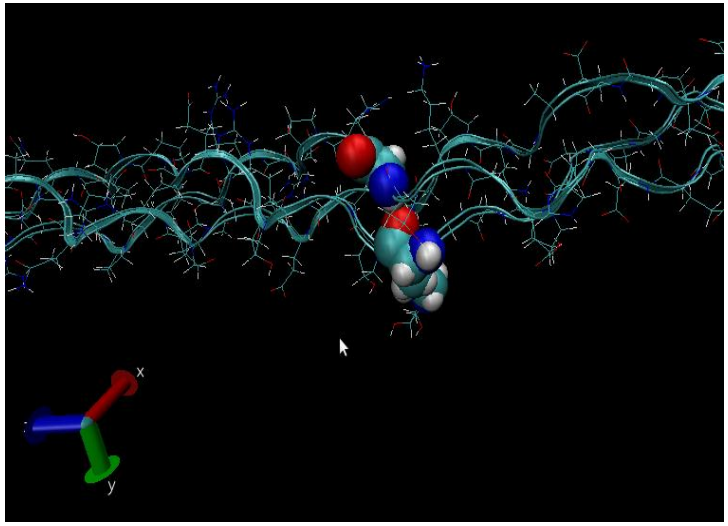

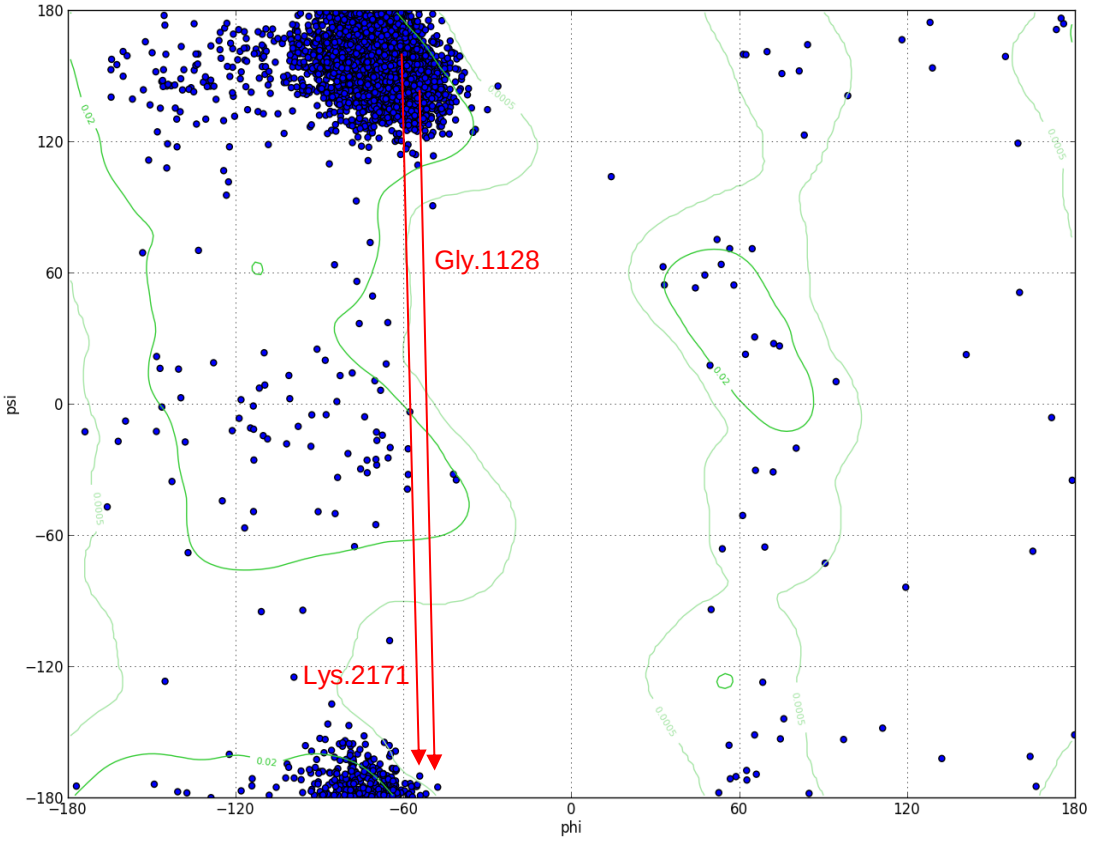

- Steric clash between Gly.1128 and Lys.2171

Position 8

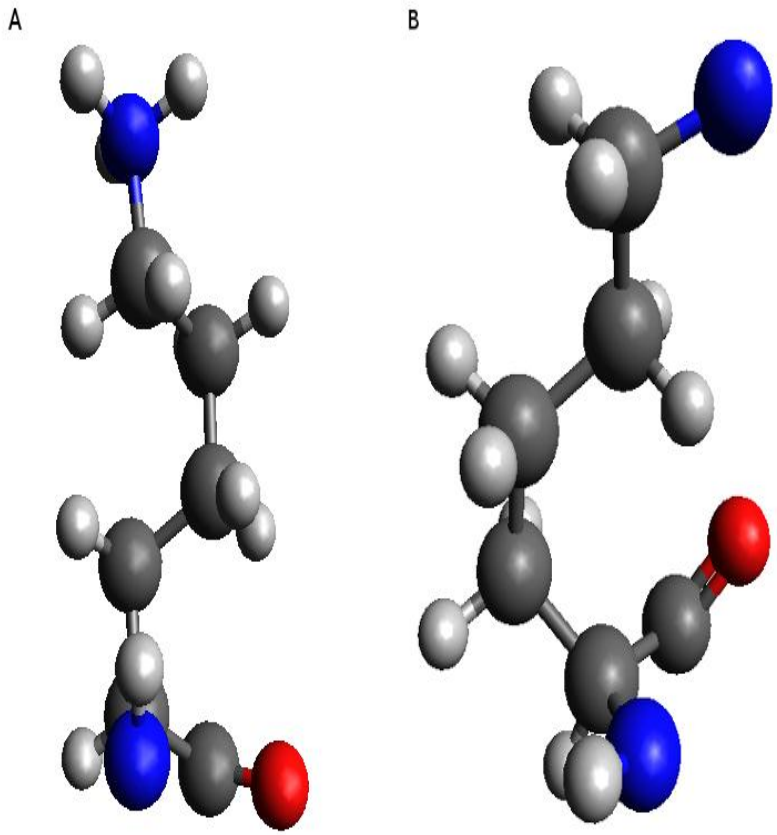

Configuration of Lys.1487 in A) unlinked collagen B) Cross-linked Collagen

- +35.702 kcal/mol

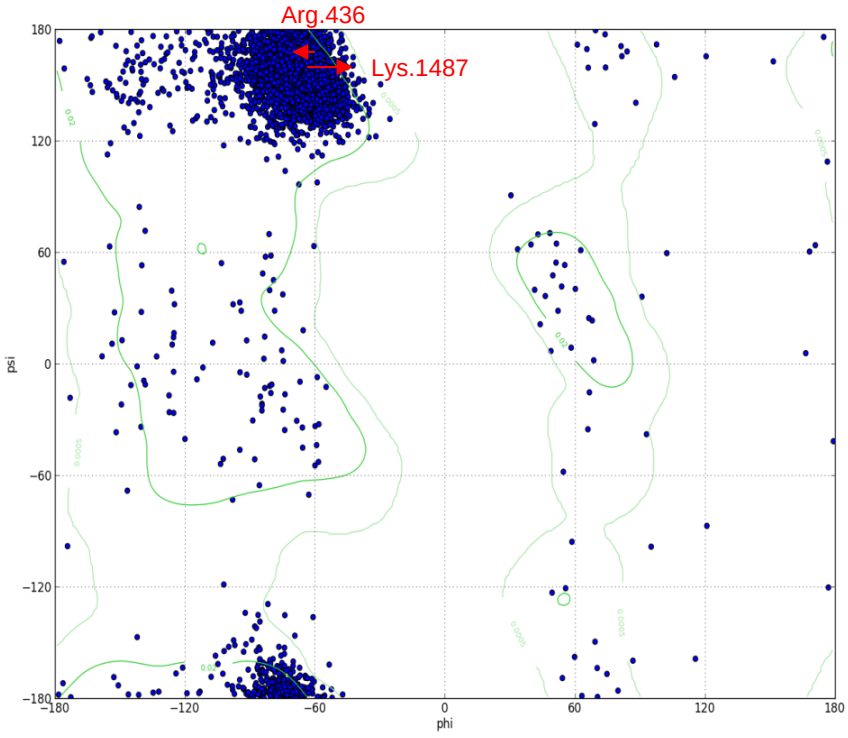

Position 10

- -91.253 kcal/mol

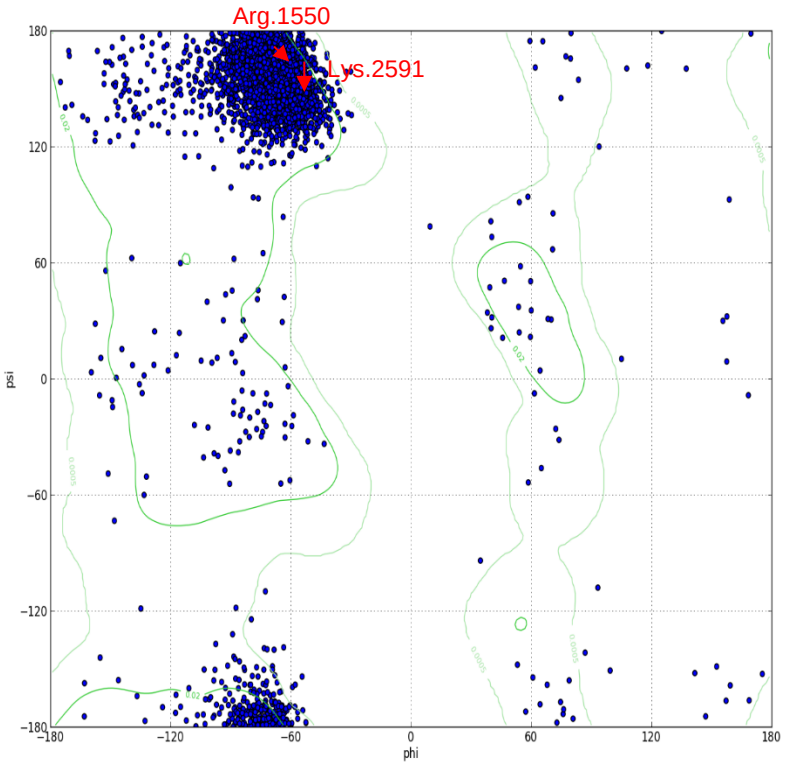

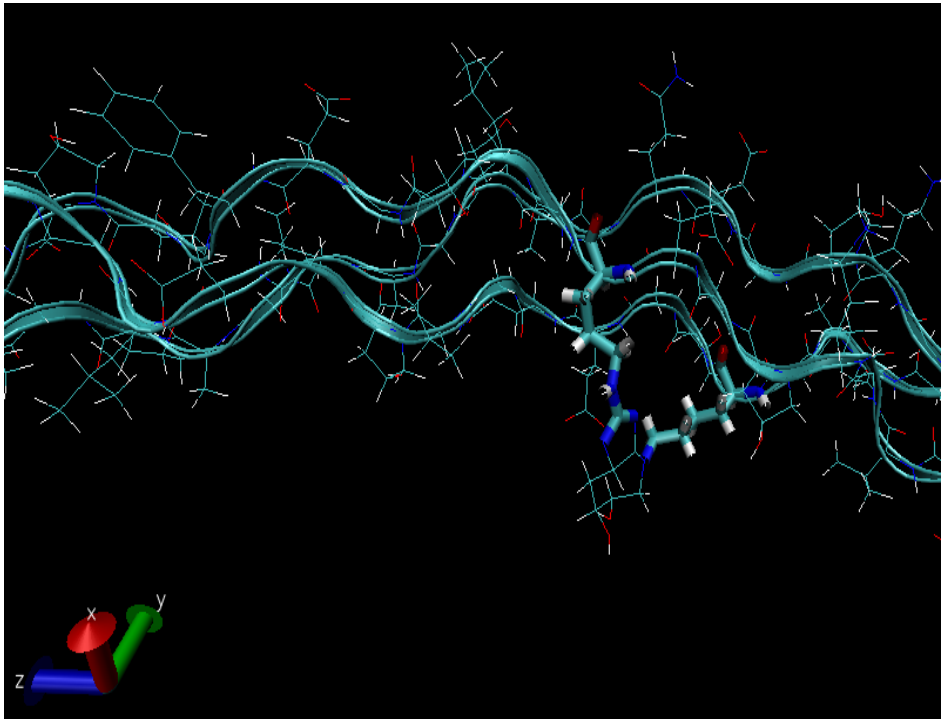

- Local conformation makes a significant effect on energy

Trends of glucosepane cross-links in collagen

- 24 Potential sites for intra-fibrillar cross-linking identified
- Glucosepane cross-linking at 11 of these sites is an exothermic process
- Using the entropy calculated in Nasiri et al.'s study 13 of these sites will have negative Gibb's free energies and thus may spontaneously form *in vivo*

R. Nasiri, M. Zahedi, H. Jamet and A.A. Moosavi-Movahedi, *J. Molecular Modelling*, 2012, **18**, 1645.

Phosphate-based Bio-active Glasses (PBGs)

- "Third generation bioactive materials"
  - Promote tissue regeneration
  - Degrade after tissue repair
- Dissolution controlled by composition
  - P_2O_5, CaO, Na_2O
  - Solubility decreases with increasing [Ca]
  - Tailored to end application
- How does composition affect glass structure?

Neural repair application

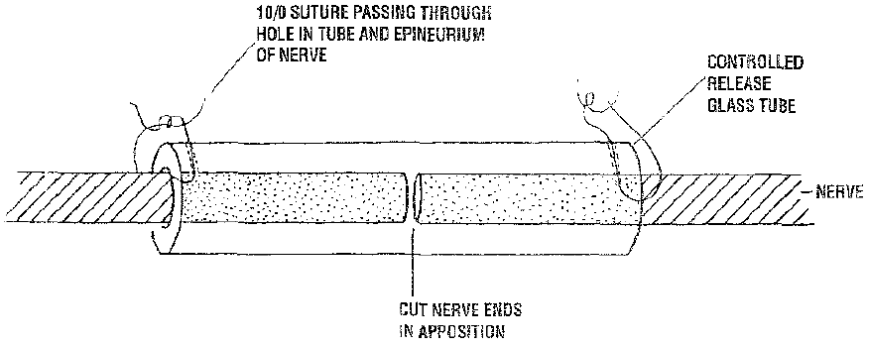

Na_2O -> CaO substitution increases durability

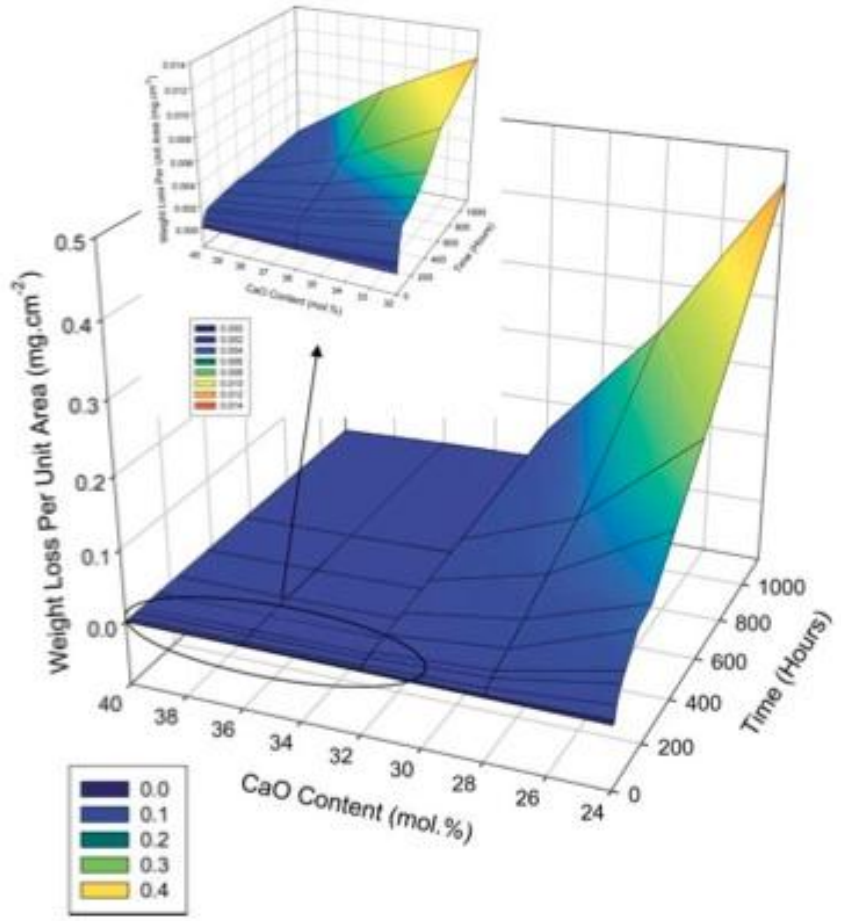

Fig. 3 Effect of CaO content on the weight loss per unit area against time between CaO content of 24 and 40 mol% and inset an enlargement of the region from 32 to 40 mol%. Reproduced with permission from ref. 14.

from J. C. Knowles, J. Mater. Chem. 2003

Compositions studied

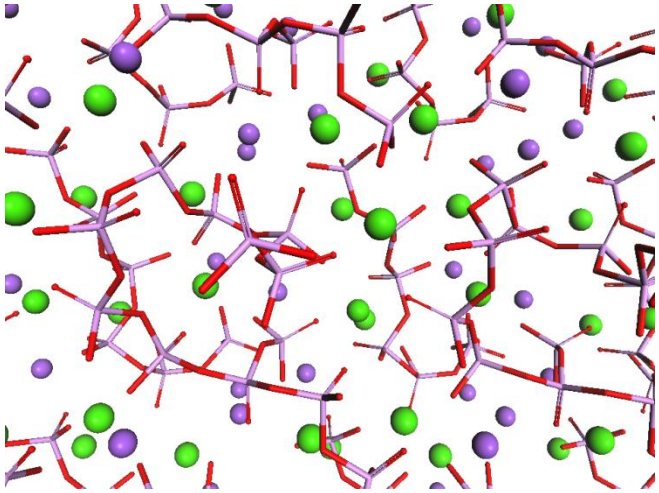

P_2O_5

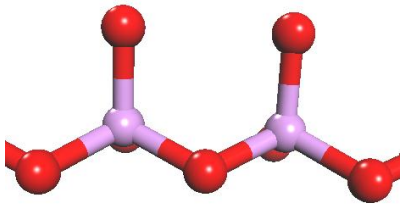

Ca

Na

$(P_2O_5)_{45}(CaO)_{30}(Na_2O)_{25}$ – P45C30N25

$(P_2O_5)_{45}(CaO)_{35}(Na_2O)_{20}$ – P45C35N20

$(P_2O_5)_{45}(CaO)_{40}(Na_2O)_{15}$ – P45C40N15

Molecular Dynamics simulations

- Ab initio MD for small samples, short time-scales
  - Short and medium-range structures
  - Electronic structures and charge densities
- Classical MD for larger samples and longer time-scales
  - Better statistics
  - Time-dependent behaviour: diffusion
- Need new forcefield for multiple compositions

Potential Derivation

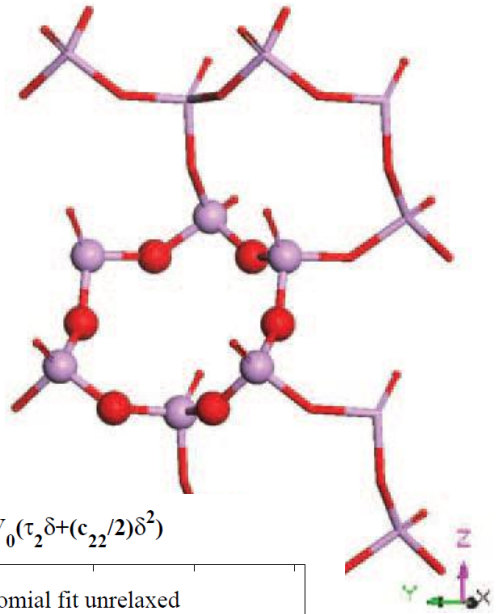

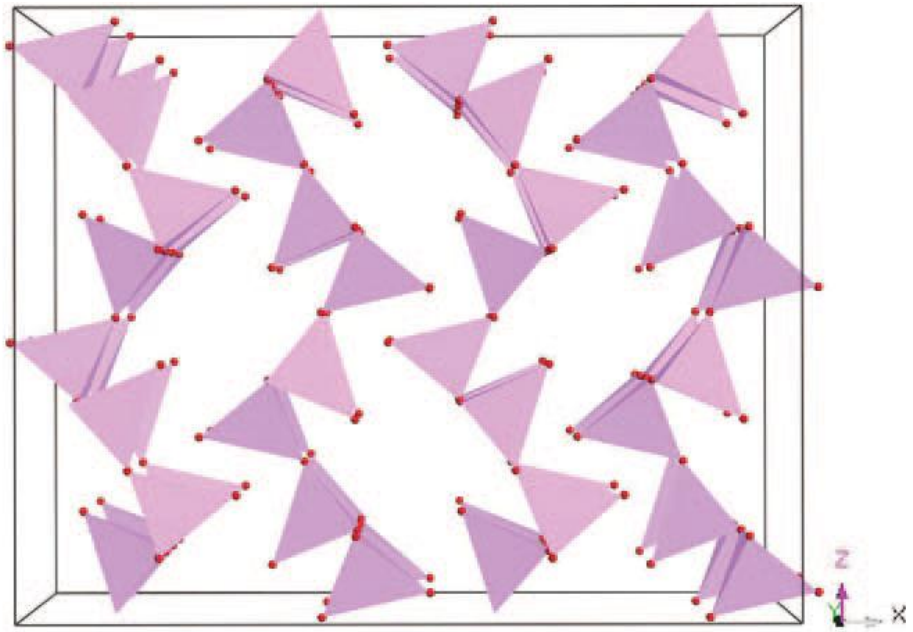

$E(V,\delta)=E(V_0,0)+V_0(\tau_2\delta+(c_{22}/2)\delta^2)$

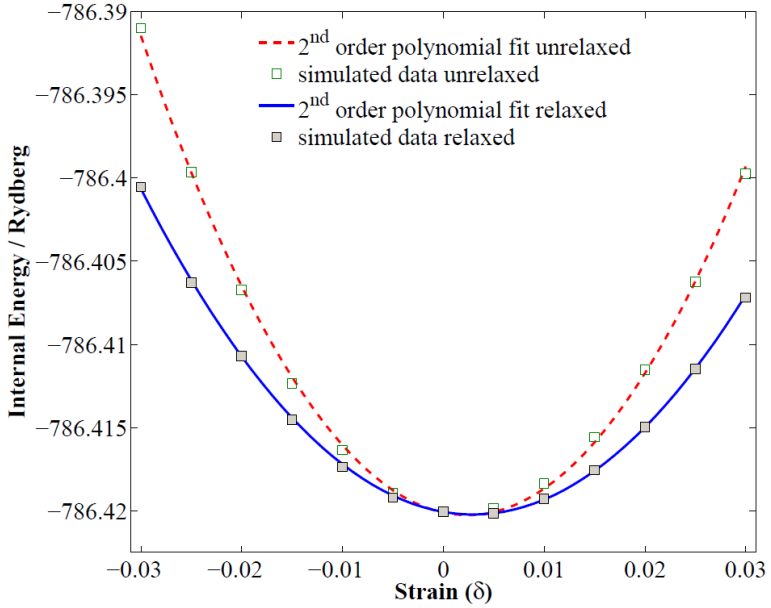

o'-$(P_2O_5)_\infty$

R.I. Ainsworth, D. Di Tommaso, N.H. de Leeuw
J. Chem. Phys. (2011) **135**, 234513

Glass generation protocol

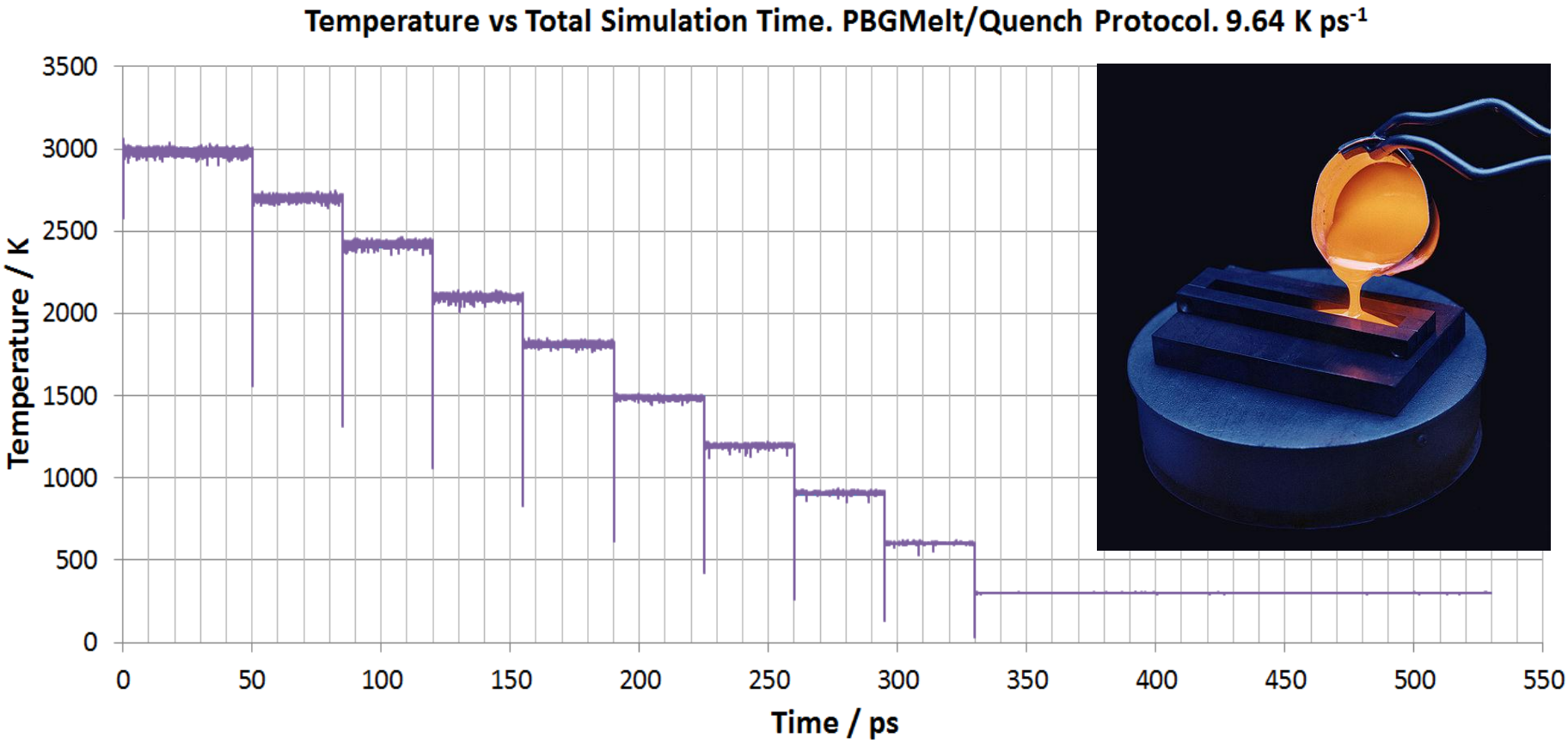

P-O Radial Distribution Function 300K

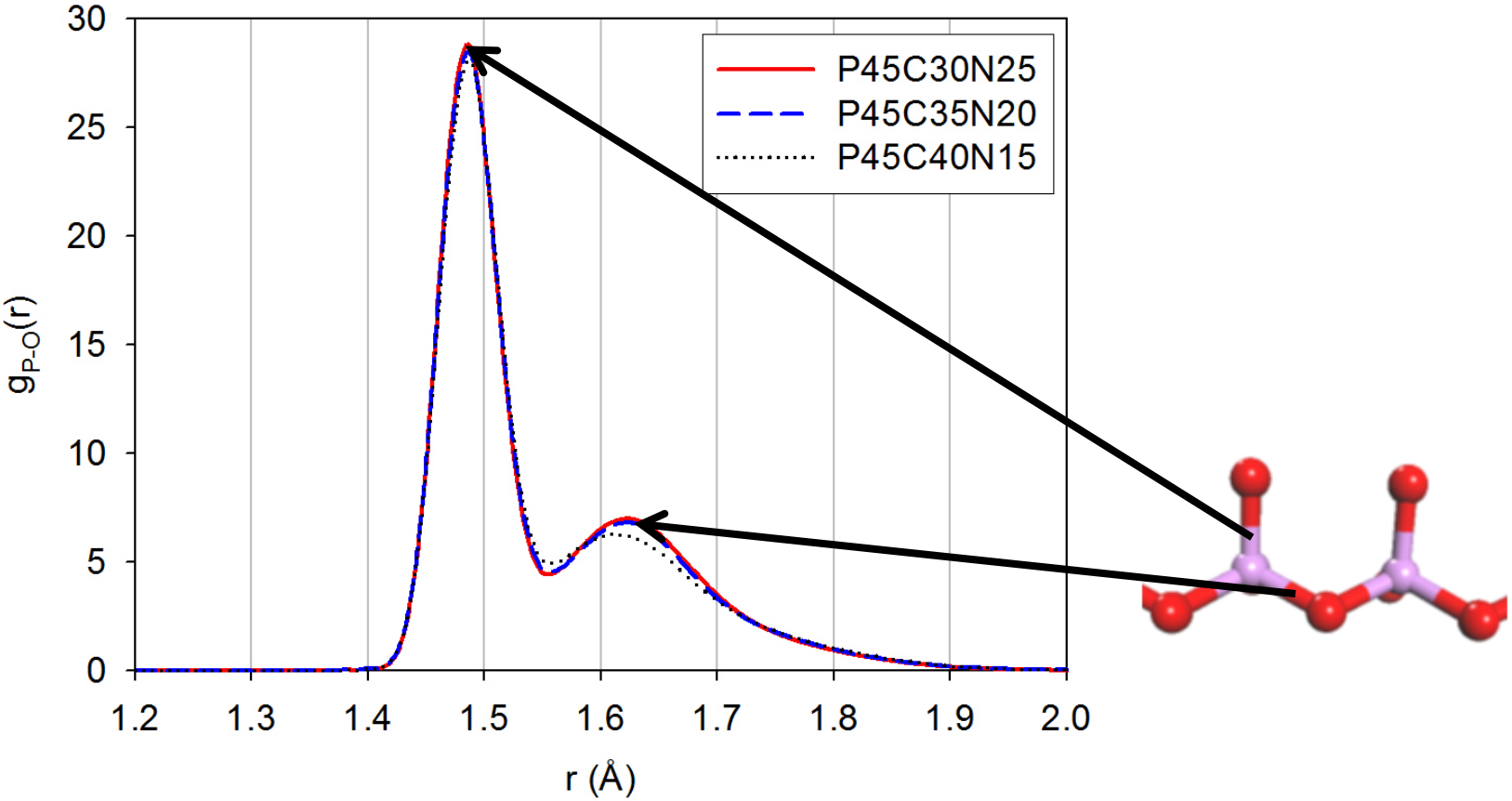

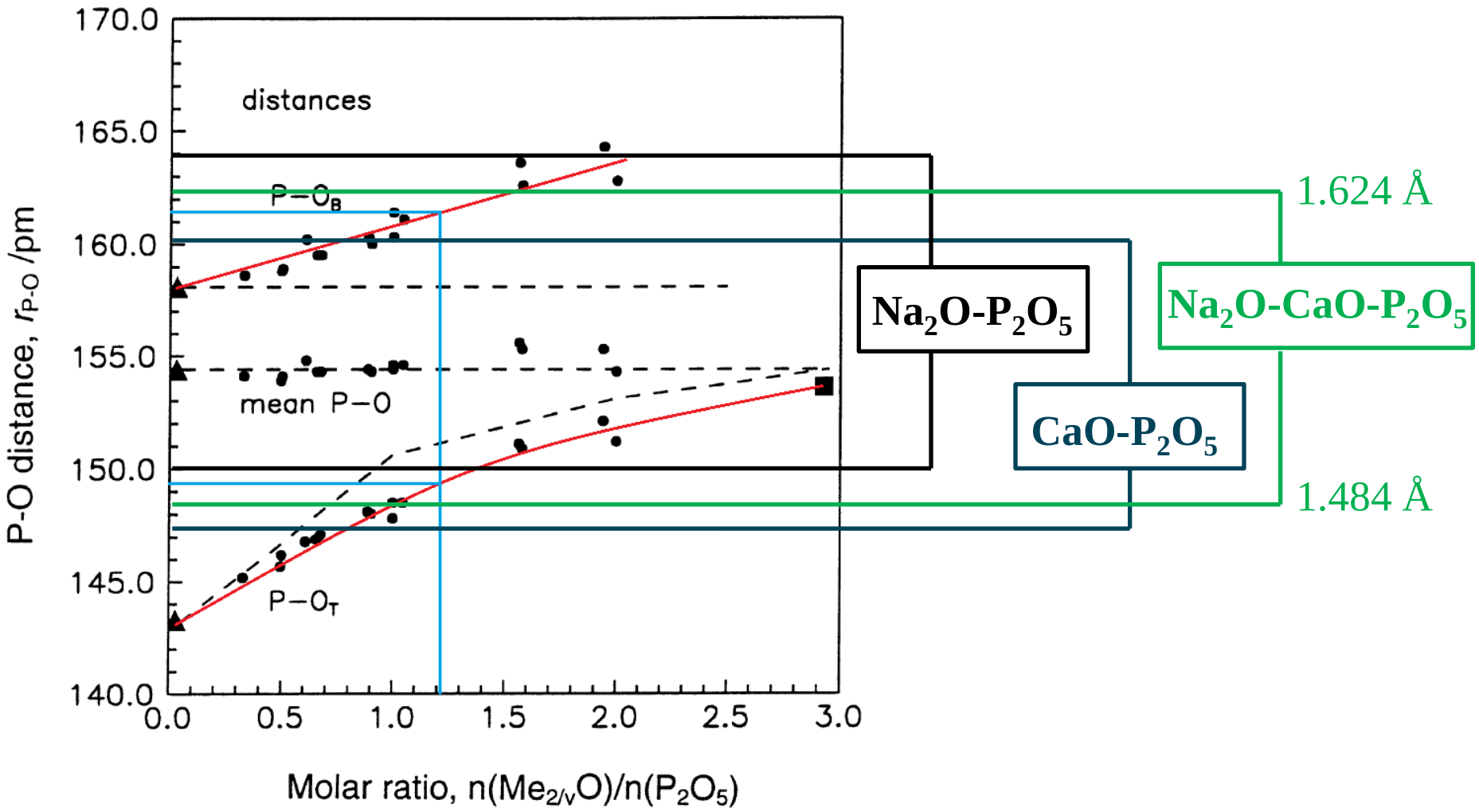

Hoppe, Walter, Kranold & Stachel. *Journal of Non-Crystalline Solids.* **263&264** 29-47 2000

Angular Distribution Functions

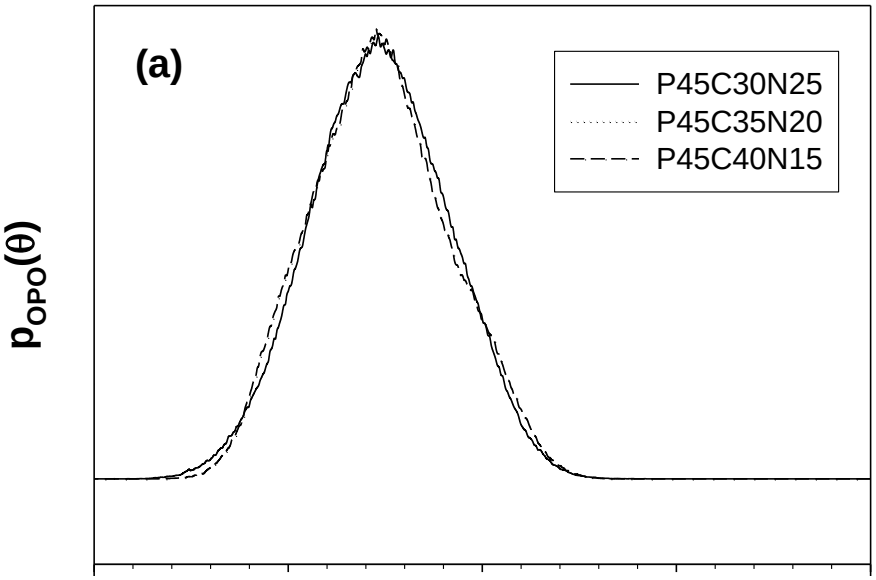

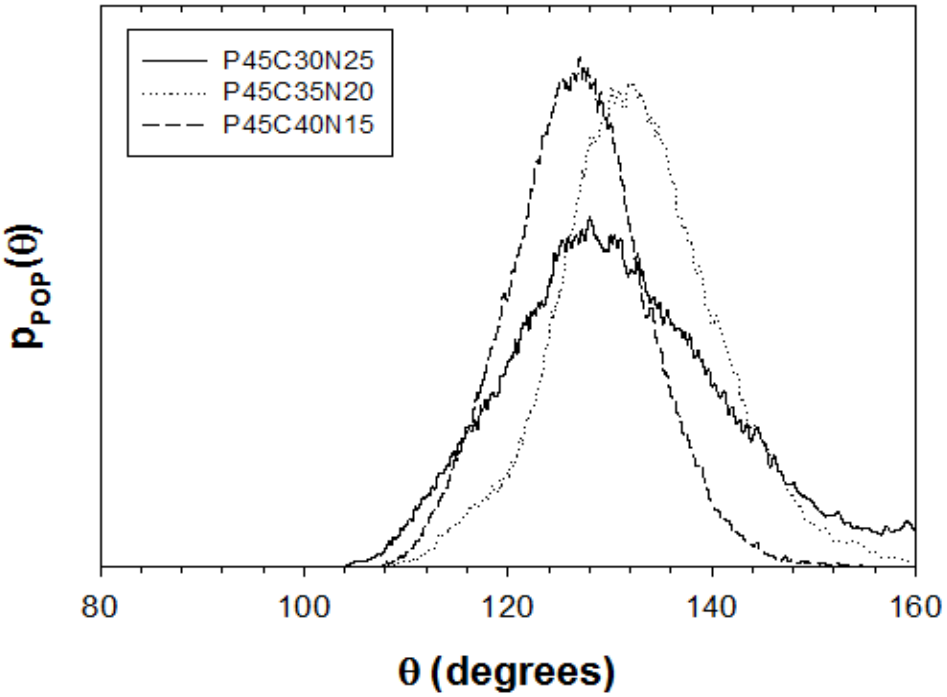

	$\frac{1}{2}k_{3b}(\theta-\theta_0)^2$	
	$k_{3b}(eVrad^{-2})$	$\theta_0(^\circ)$
O_s-P-O_s	3.3588	109.470000
P-O_s-P	7.6346	141.179333

E. Tang, D. Di Tommaso, N.H. de Leeuw, *Adv. Eng. Mater.* (2010) **12**, B331.

Short-range Structural Summary

	P45C30N25 this work	P45C35N20 this work	P45C40N15 this work	P60C40 [3] ND & XRD	P50N50 [4] XRD	P45C30N25 [5] XRD	P50C40N10 [6] ND & NMR
$r_{(P=O)}$	1.485	1.486	1.487	1.475	1.50 ±0.025	1.52 ± 0.02	1.49 ± 0.02
$r_{(P-O)}$	1.623	1.622	1.613	1.600	1.64 ±0.025	1.60 ± 0.02	1.60 ± 0.02
$r_{(O-O)}$	2.543	2.543	2.543	2.525		2.54 ± 0.02	2.52 ± 0.02
$r_{(P-P)}$	3.040	3.041	3.039			2.95 ± 0.02	2.93 ± 0.02
$r_{(Na-O)}$	2.353	2.371	2.363			2.41 ± 0.02	2.33 ± 0.02
$r_{(Ca-O)}$	2.334	2.333	2.329	2.345		2.40 ± 0.02	2.34 ± 0.02
$\theta_{(O-P-O)}$	108.65	108.67	108.99				
$\theta_{(P-O-P)}$	134.50	134.56	134.52		130		

3. Hoppe *et al. Short-range order in ultraphosphate glasses.* Physica B, 1997. **234** (388–390).
4. Suzuki & Ueno. *Experimental discrimination between bridging and nonbridging oxygen phosphorus bonds in p2o5,na2o glass by pulsed neutron total scattering.* Journal de Physique, 1985. **46** (261-265).
5. Carta *et al. A structural study of sol-gel and melt-quenched phosphate-based glasses.* Journal of Non-Crystalline Solids, 2007. **353**(18-21) (1759-1765).
6. Pickup *et al. The structure of phosphate glass biomaterials from neutron diffraction and p31 nuclear magnetic resonance data.* Journal of Physics: Condensed Matter, 2007. **19**(41).

Medium-range structure: Q^n

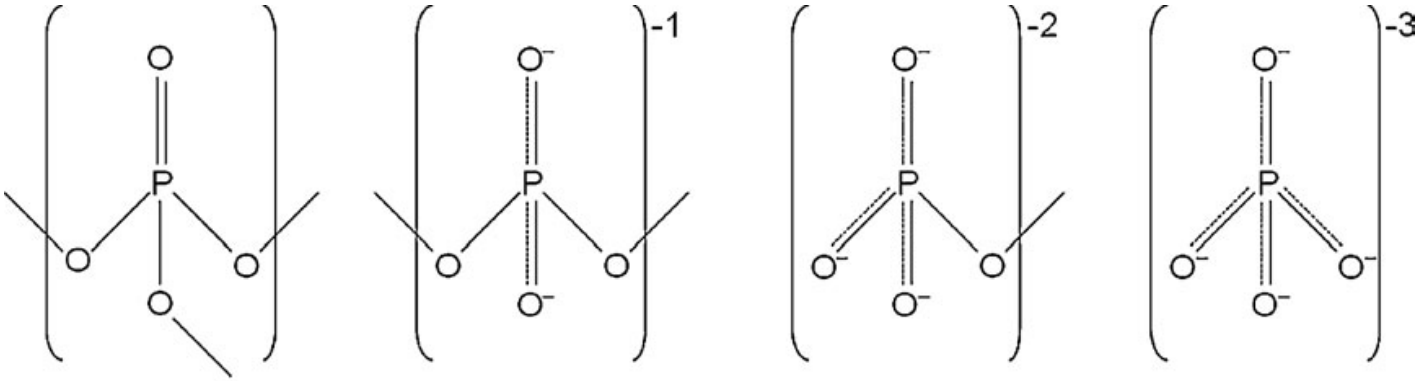

	Q^0	Q^1	Q^2	Q^3	Q^4	NC	P_c	Q^1 [5]	Q^2 [5]
P45C30N25	0.0	25.9	70.1	4.0	0.0	1.78	4.0	22 ±2	78 ±2
P45C35N20	0.0	27.7	67.0	5.1	0.2	1.78	4.0	21 ±2	79 ±2
P45C40N15	0.0	28.7	64.6	6.7	0.0	1.78	4.0	10 ±2	90 ±2

5. Carta *et al. A structural study of sol-gel and melt-quenched phosphate-based glasses.* Journal of Non-Crystalline Solids, 2007. **353**(18-21) (1759-1765).

Medium-range structure: Coordination Number

	P45C30N25	P45C35N20	P45C40N15
Atomic Pair	CN	CN	CN
Na-O	6.49	6.59	6.57
Na-BO	1.26	1.30	1.32
Na-NBO	5.23	5.29	5.25
CN^{Na-NBO}/CN^{Na-BO}	4.15	4.07	3.98
Ca-O	6.86	6.82	6.87
Ca-BO	0.59	0.55	0.62
Ca-NBO	6.27	6.27	6.25
CN^{Ca-NBO}/CN^{Ca-BO}	10.63	11.40	10.08

Table. Modifier coordination environments. Na-O and Ca-O cutoffs set at 3.15 Å and 3.22 Å respectively.

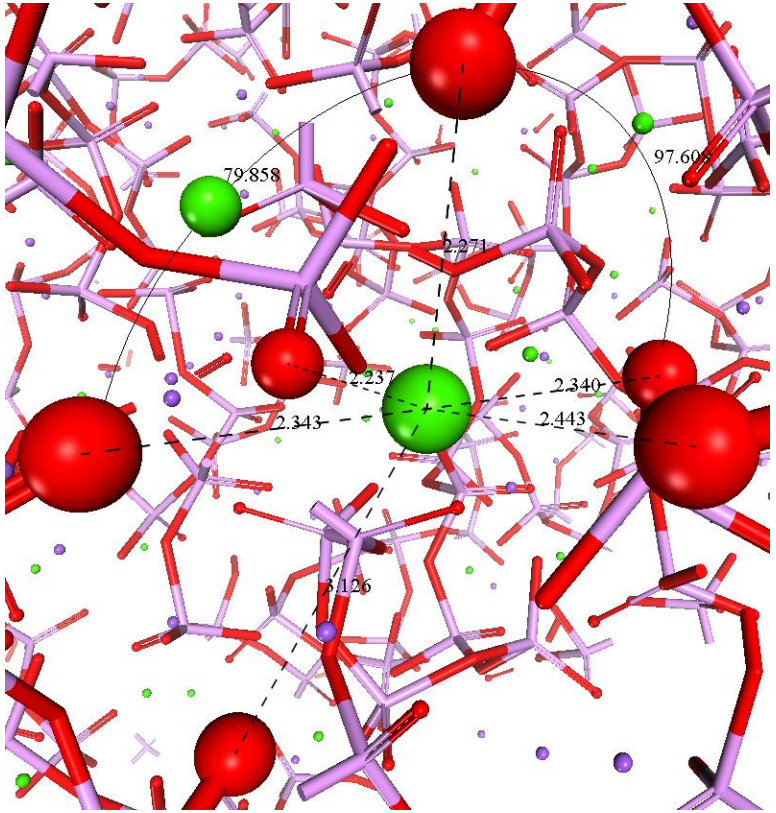

Figure. Ca^{2+} pseudo-octahedral coordination shell. Snapshot from P45C35N20 trajectory at 300K.

Fragments

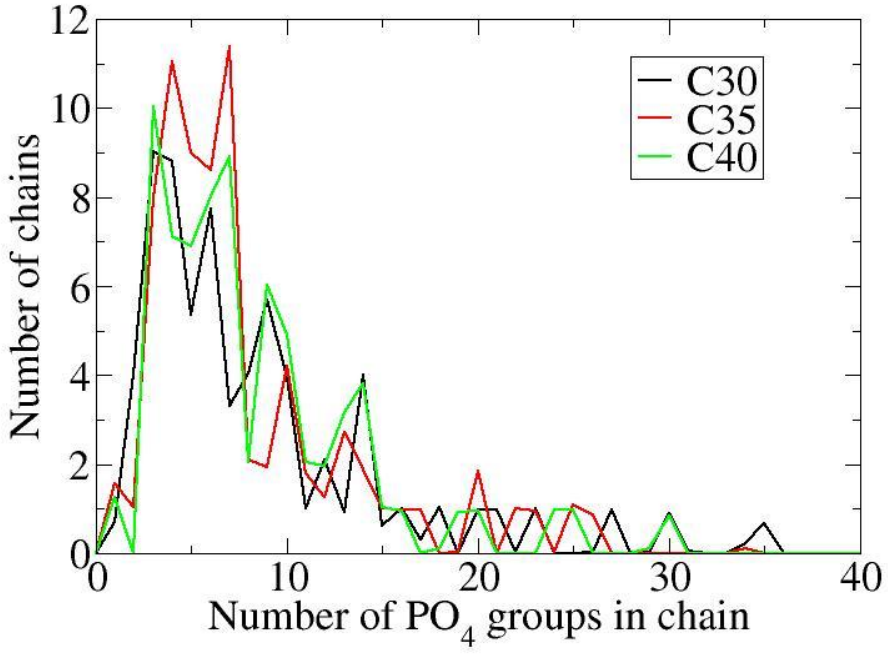

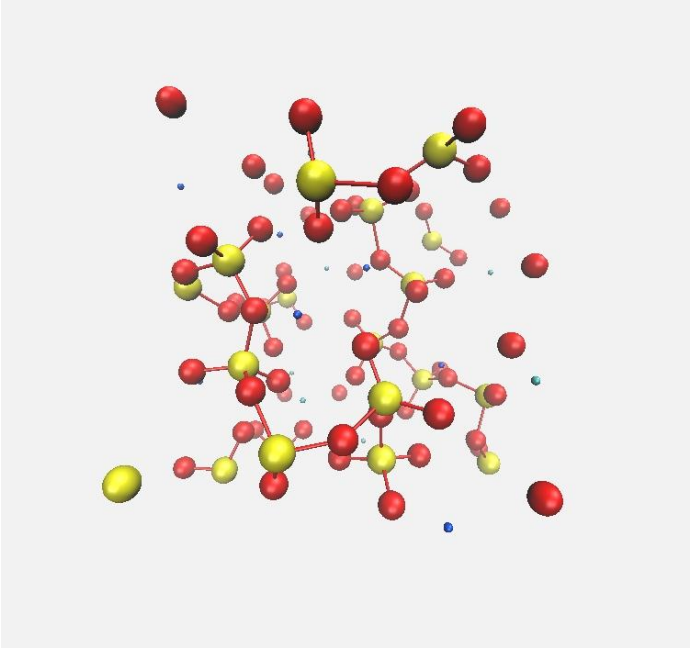

Chain-length distribution does not depend on Na/Ca composition

Structures around modifier cations

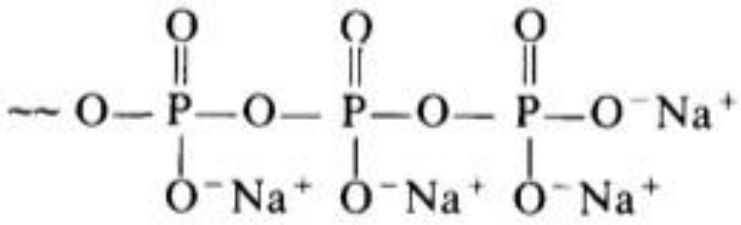

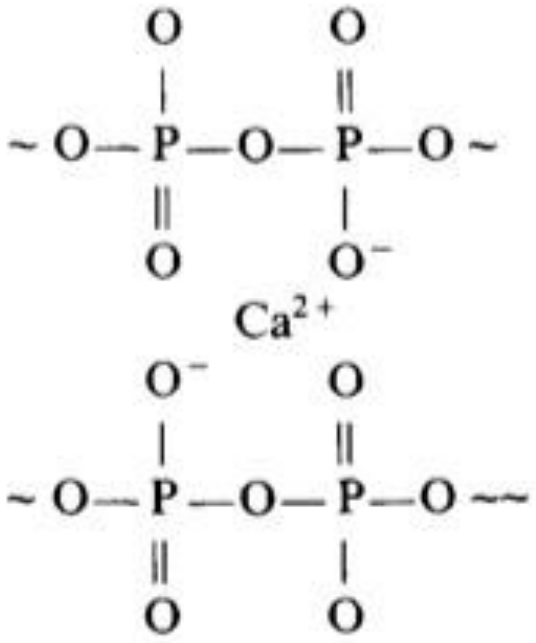

from Bunker et al., J. Non-Cryst. Sols. 1984

Suggestions

- Ca^{2+} cross-links chains, Na^{+} does not
- Difficult to reconcile with pictures from diffraction / spectroscopy

Ca/Na binding behaviour

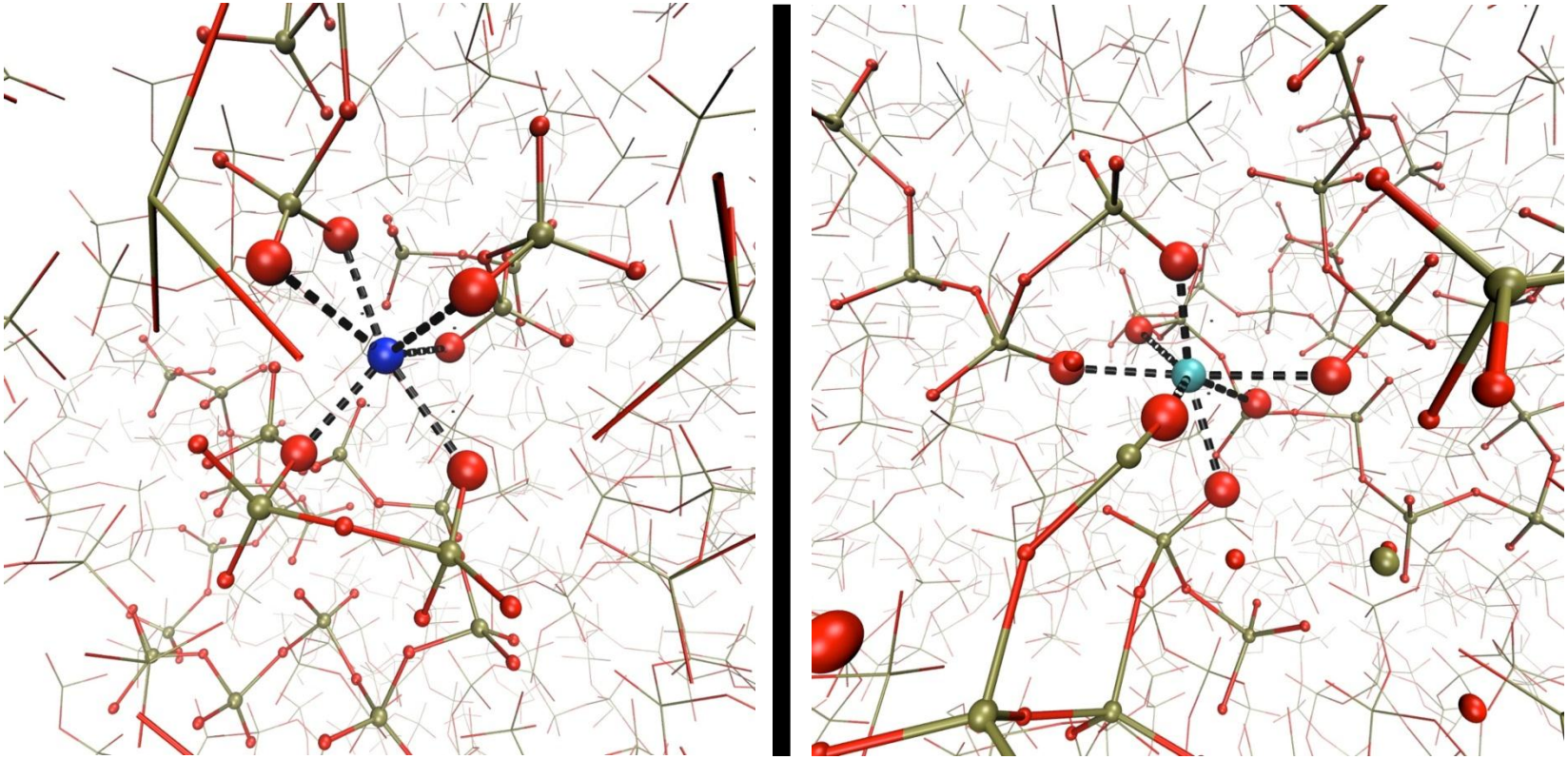

Na bound to
3.2 fragments

Ca bound to
3.9 fragments

Medium-range structure: Cross linking

	Fragments	μ_{frag}^{Na}	μ_{frag}^{Ca}
P45C30N25	69.7	3.25	3.85
P45C35N20	75.5	3.28	3.96
P45C40N15	73.3	3.24	3.92

Table. Number of phosphate network fragments. Mean number of fragments bound to a modifier.

- Solely chain-like network fragments with no ring structures in agreement with theory for P≤50.
- Ca “cross-links” more fragments than Na.

J. Christie, R.I. Ainsworth, D. Di Tommaso, N.H. de Leeuw, *J. Phys. Chem. B* (2013)

Summary: Structural links to dissolution

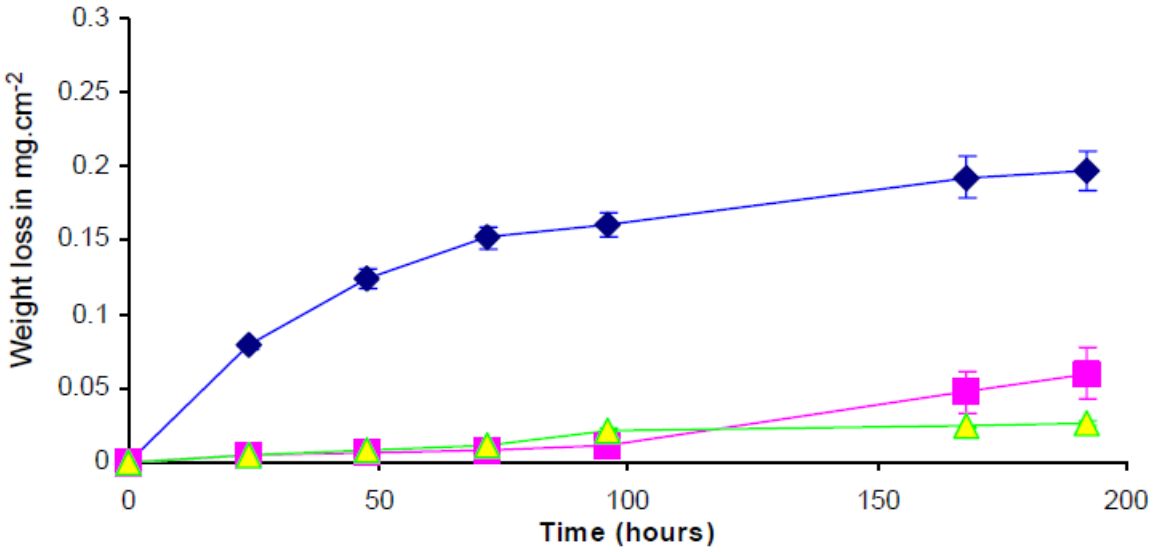

Ahmed, Lewis, Olsen & Knowles. *Biomaterials*. **25** 491-499 2004

[◆ = 30 mol% CaO, ■ = 35 mol% CaO, △ = 40 mol% CaO]

- Ca bonds to more oxygen within first coordination shell than Na
- Ca forms more bonds to NBO compared with Na
- Ca increases rigidity of PBG structure
- Ca "cross-links" more fragments than Na

Titanium-doped PBGs

- Ti affects degradability of glass and other properties
- Ti elicits favourable cell response

Simulated Compositions:

$$(P_2O_5)_{45}(CaO)_{30}(Na_2O)_{25} - P45C30N25$$

$$(P_2O_5)_{45}(CaO)_{30}(Na_2O)_{10}(TiO_2)_{15} - P45C30N10T15$$

Ti-doped PBG: Short-range Structure

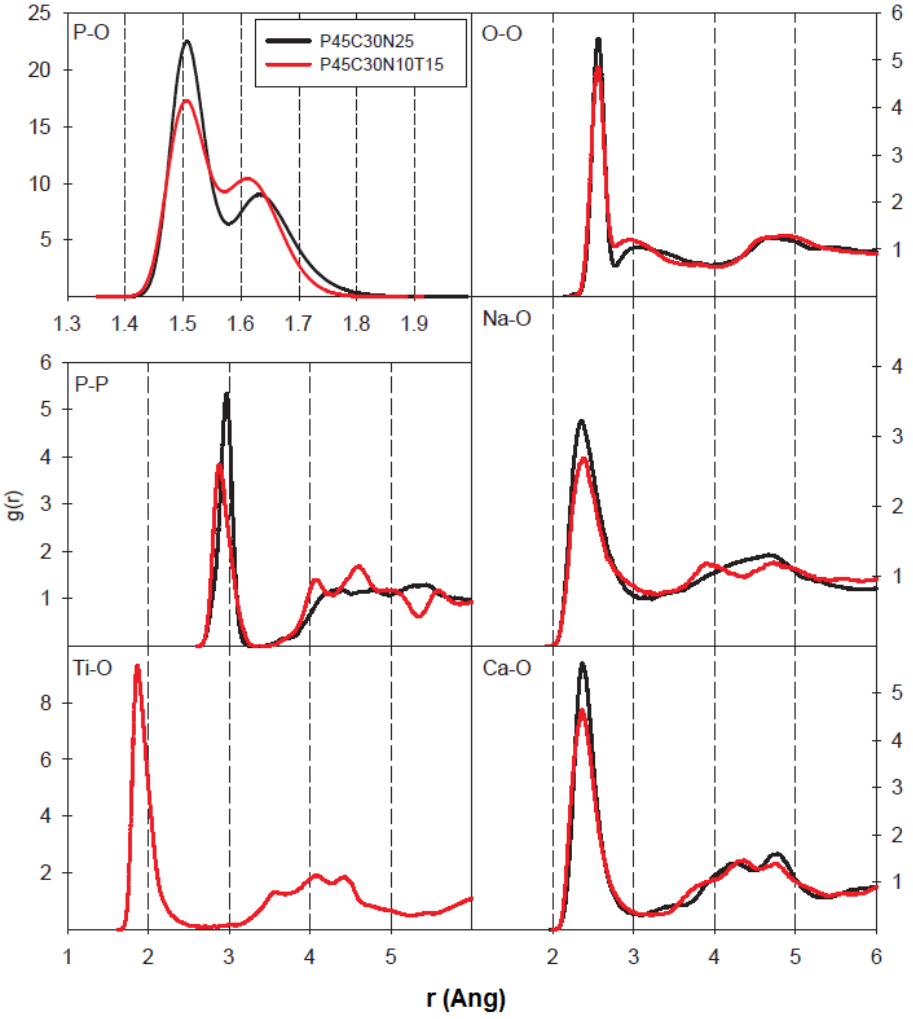

TABLE V: Q^n species distribution (%) for phosphorus with respect to oxygen and network connectivity (NC). P45C30N10T15 results for phosphorus Q^n species distribution including$_{(i)}$ and excluding$_{(e)}$ P-BO-Ti contributions. Experimental NMR results[1]given for comparison. P-O and Ti-O cut-offs set at 2.0 and 2.8 Å respectively.

	Q^0	Q^1	Q^2	Q^3	Q^4	NC	Q^1[1]	Q^2[1]
P45C30N25	0.0	25.0	70.0	5.0	0.0	1.80	22 ±1	78 ±1
P45C30N10T15$_i$	0.0	5.0	58.2	29.3	7.5	2.39	5 ±1	95 ±1
P45C30N10T15$_e$	10.0	30.0	55.0	5.0	0.0	1.55		

87.5% cf. 95%

Ti-doped PBG: NMR Spectra

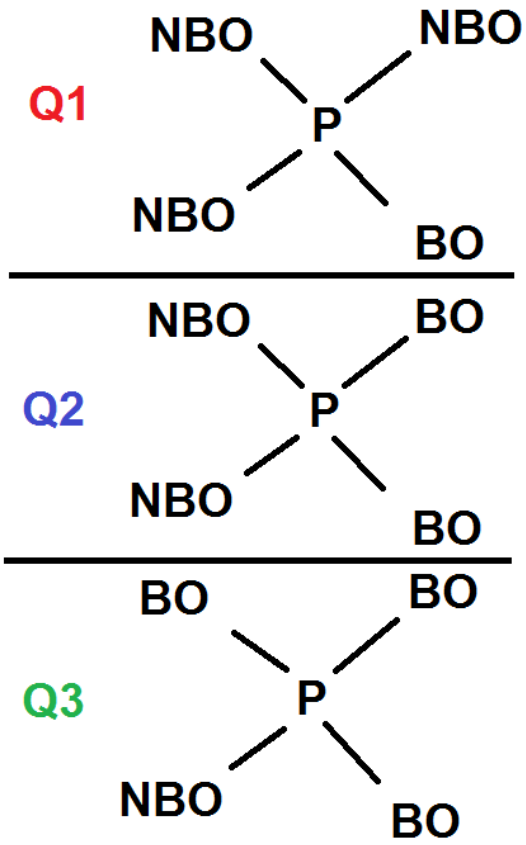

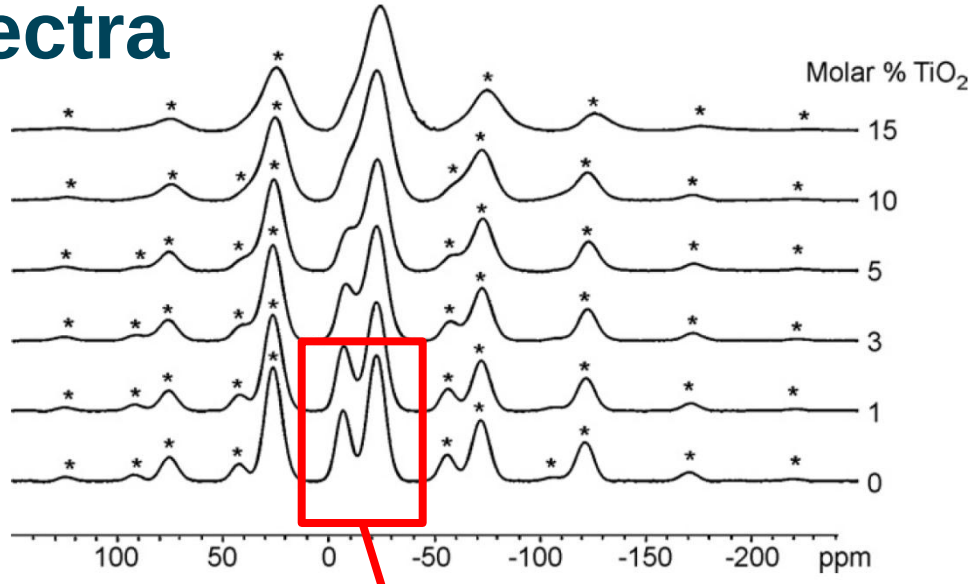

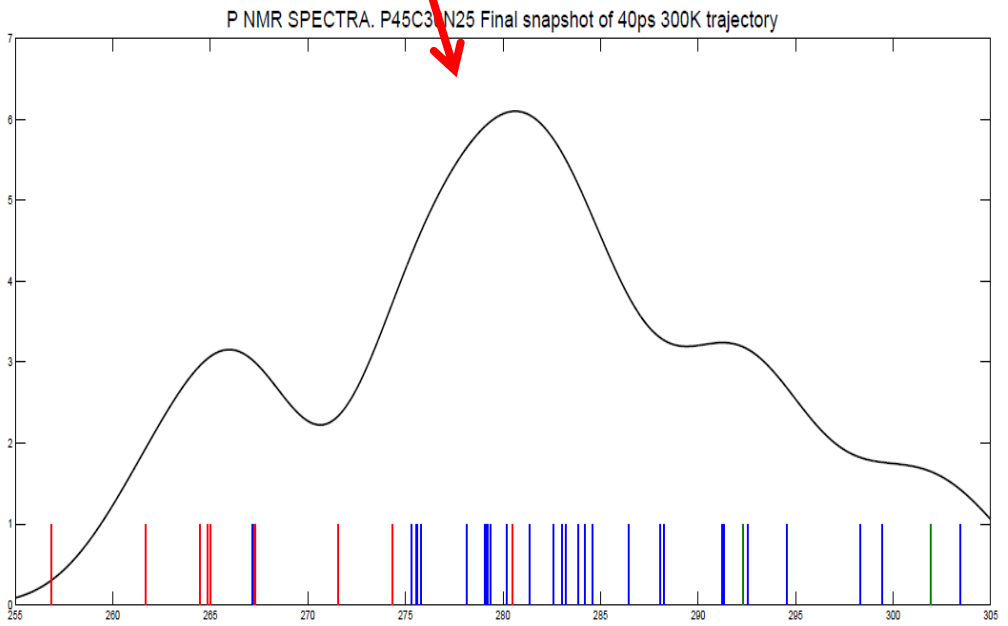

PBG Summary

- Ti is a network intermediate and might flip between tetrahedral / octahedral
  - Ti-BO-Ti-NBO
- Ti acts as network former
- More Q^3 in simulation than in experimental NMR
- $[Q^2+Q^3]$ agrees with experiment

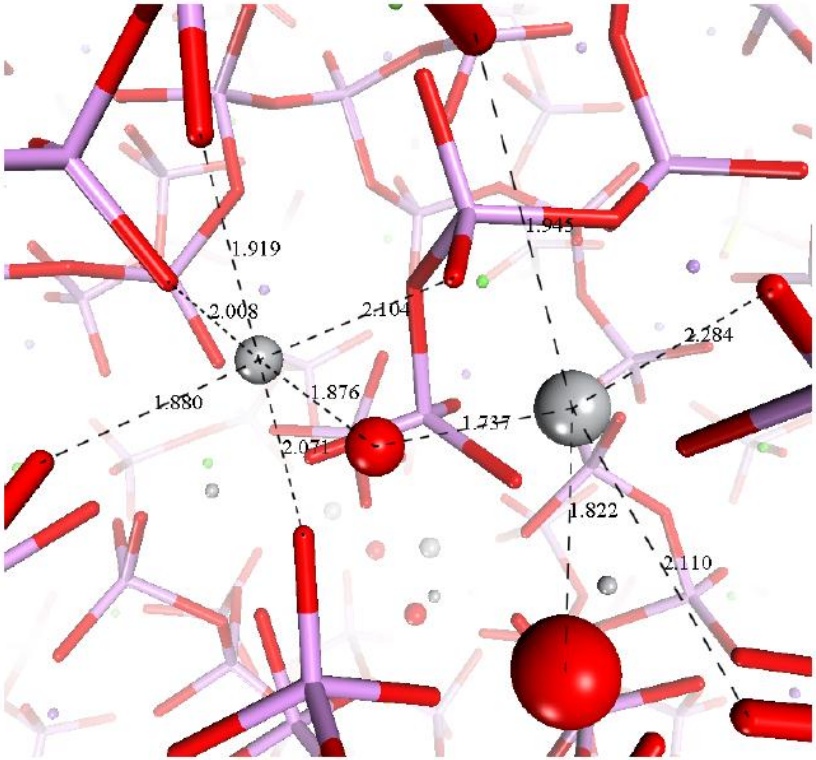

FIG. 2: Snapshot of P45C30N10T15 300 K MD

Acknowledgements

Neyvis Almora-Barrios

Sergio Ruiz-Hernandez

Ian Streeter

Tom Collier

Jamieson Christie

Richard Ainsworth